Assessing the Potential Impact of Climate Change on the Surface Hydrology of Prince Edward Island

by

Shane Warner

Submitted in partial fulfilment of the requirements

for the degree of

MASTER OF APPLIED SCIENCE

at

Dalhousie University

Halifax, Nova Scotia

October 2016

Table of Contents

List of Tables

List of Figures

Abstract

This study used the HBV hydrological model to assess the potential impact of climate change on five watersheds on Prince Edward Island, Canada. The model was successfully constructed and calibrated using a 2000 run Monte Carlo simulation. One parameter set was found to produce satisfactory simulations for three of the six catchments, suggesting that the physical characteristics of the watersheds are similar.

Six climate scenarios comprising three emission scenarios and four global coupled models were used as model input to assess potential climate change impacts on the hydrological system for the period 1985 - 2044. Overall, most components of the hydrological system showed little to moderate change. Mean annual drainage increases by 8% in the most likely scenario, but increases up to 23% in wetter scenarios. Seasonally, the increased flow is shown to occur in the winter (+38%), while spring melt flows drop by 12% and summer flows show little change (+7%). Fall flows increase in wetter scenarios (up to +33%) but drop in drier ones (-12%). Annual flow indicators (Q10, Q50, Q90) remain stable in the base-case scenario, but show small, steady increases in all other scenarios. Assessment of summer drought severity shows that there is little change to both the 7Q10 and 60Q50 droughts.

Analysis of the annual water balance components showed some larger changes. While the runoff coefficient is steady around 0.6 and evapotranspiration shows a minor increase in all scenarios, net recharge to deep groundwater decreases by at least 15% and up to 60% in the base-case scenario. Winter snowpack volumes also decrease between -40% and -71% in the last decade of simulation in all scenarios.

Overall, change values between historic and future periods from the six simulations agree in direction for nearly all results, and show only moderate variation (generally less than 30 percentage points) in magnitude. This indicates that the impact of climate change on the hydrological system in Prince Edward Island is relatively well constrained.

List of Abbreviations Used

60Q50	Minimum sixty-day average flow expected once in fifty years
7Q10	Minimum seven-day average flow expected once in ten years
AAFC	Agriculture and Agri-Foods Canada
AET	Actual Evapotranspiration
AR5	5th Assessment report of the IPCC
BCCAQ	Bias correction constructed analogues with quantile mapping
BCSD	Bias correction/spatial downscaling
BCSDX	Bias correction/spatial downscaling using minimum/maximum temperature
CA	Constructed analogues
CMIP5	Coupled Model Intercomparison Project 5
DEM	Digital Elevation Model
ET	Evapotranspiration
GCM	Global Climate Model
GEV	General Extreme Value
HBV	Hydrologiska Byråns Vattenbalansavdelning
HRU	Hydrological Response Unit
IDU	Integrated Decision Unit
IPCC	Intergovernmental Panel on Climate Change
K-S	Kolmogorov-Smirnov value
LULC	Land use/Land cover
n	Manning's roughness coefficient
NRBF	Normalized Reference Base Flow
NSE	Nash-Sutcliffe Efficiency
NSE_{ln}	Nash-Sutcliffe Efficiency of logarithm of flow
OBJ	Objective function
PBIAS	Percent Bias
PEI	Prince Edward Island
PET	Potential Evapotranspiration
Q10	Flow exceeded 10% of the time

Q50	Flow exceeded 50% of the time (median)
Q90	Flow exceeded 90% of the time
R^2	Coefficient of Determination
RCP	Representative Concentration Pathways
SCS	Soil Conservation Service of the United States Department of Agriculture
SWAT	Soil Water Assessment Tool
SWE	Snow Water Equivalent
WSC	Water Survey of Canada

Acknowledgements

I would first like to thank my supervisor, Dr. Rob Jamieson, for all of his support throughout this project. Right from inception to final submission, you've been there to answer any questions I've had, while giving me the space and flexibility to do this project the way I wanted. You've made this whole process so much easier than I had expected, and it's been a real pleasure working with you!

Special thanks also go to Dan MacDonald, Ruth Waldick, Scott Mitchell and the rest of the Farms to Regions project team. It's been a pleasure working with you all and you've given me the opportunity to see how a complex, multi-disciplinary project can run and the benefits that can come from it. I would also like to specifically acknowledge the financial support from AAFC that made this degree possible for me – thank you.

I would like to thank Dr. John Bolte and Dr. Kellie Vache for their many hours of building new features and debugging my models and the Envision code to ensure that in the end, Envision worked for me so that I could do this project.

I would also like to thank Guy Leger with Environment and Climate Change Canada and Richard MacEwen with the Water and Sewer Utility of the City of Charlottetown for providing me with key data needed for this project.

Finally, I'd like to thank my family and friends for all their support and encouragement through this process, particularly Chaiti for trying to follow what I was doing with "the polygons" and listening to me describe the details of whatever issue I was currently facing, and Kaira for waiting until I was done.

Chapter 1 Introduction

1.1 Background

Agriculture is very important to the economy of Prince Edward Island (PEI), being both the largest employer and largest industry by GDP (PEI Agriculture, 2014). However, the productivity and sustainability of agricultural systems are at serious risk due to climate change. Policy options for adaptation and mitigation measures need to be investigated and tested to assess how effective they may be.

The Farms to Regions program at Agriculture and Agri-Food Canada (AAFC) was developed with the goal of addressing climate change at the level of strategic planning, policy design and implementation across sectors and jurisdictions through adaptation (Waldick, 2011). One of the specific objectives was to develop scenarios for future conditions and practices that affect agriculture and assess the outcomes using multi-sector modeling. Pilot work under the Farms to Regions program integrated preliminary population, crop allocation, nutrient runoff and wildlife habitat models, however further work was needed to properly address all of the critical processes related to agriculture.

Hydrology is intimately tied to agriculture, with soil moisture being a critical water source for crop growth and surface water being both an important source of irrigation and a major sink for sediment and nutrient runoff. Quantification of these water volumes and fluxes allows for more accurate crop growth, nutrient runoff and wildlife habitat models, as well as directly quantifying stream flows to assess environmental minimum flows, potential irrigation supplies as well as flood risk. For these reasons, it was important to add a hydrological model to the Farms to Regions modeling suite. Hydrological modelling uses geospatial and climate data to simulate watersheds and calculate water contents and fluxes throughout the system. Recent initiatives at the provincial and national level in Canada have produced detailed spatial data (e.g. topography, land use/land cover, crop distribution, soils) that can be used to better describe watershed conditions. New climate models from the 5th Assessment Report of the Intergovernmental Panel on Climate Change (IPCC) are now available and

downscaled climate datasets appropriate for local/regional models have been produced for the region (Pacific Climate Impact Consortium, 2014). These new datasets can be used to drive spatially explicit hydrological models that assess the characteristics and responses of individual watersheds.

Prince Edward Island was selected as a focus region for further development and expansion of the Farms to Regions program. Given current issues related to water availability for agriculture and impacts of agricultural runoff on aquatic ecosystems in PEI, the western portion of PEI encompassing the primary agricultural regions was selected as the study area for development of the Farms to Regions hydrological model.

1.2 Study Objectives

The overall objective of this study is to evaluate the use of the HBV hydrological model in simulating the potential impact of climate change on stream flows in PEI. Specific objectives included:

- Construction, calibration and validation of the HBV hydrological model for PEI watersheds.
- Assessment of the potential impact of climate change on stream flows and water budgets in PEI watersheds.

Chapter 2 Literature Review

2.1 Climate Change Projections

The IPCC released its fifth annual report in 2014 (IPCC, 2014). This report builds upon the Coupled Model Intercomparison Project 5 (CMIP5) which aims to produce comparable results from over 50 world-leading Global Climate Models (GCMs) (Taylor, Stouffer & Meehl, 2012). In addition to new and revised GCMs, AR5 introduces four new future climate scenarios based on Representative Concentration Pathways (RCPs): RCP2.6, RCP4.5, RCP6.0 and RCP8.5. RCP8.5 is the high greenhouse gas emission scenario reflective of what may occur with no limiting of anthropogenic emissions, while RCP2.6 incorporates stringent reductions in emissions that would be required to likely avoid 2˚C of warming. RCP4.5 and RCP6 are intermediate scenarios with different timelines and levels of emission reduction (IPCC, 2014).

Maloney et al. (2014) reviewed seventeen GCMs that were part of the CMIP5 project and reported changes between 1961-1990 and 2070-2099 for the RCP8.5 emission scenario. For Atlantic Canada, they found that on average, temperatures are expected to increase by approximately 5˚C in both summer and winter, while precipitation will increase slightly (0 – 0.25 mm/day, ≈5%) in the summer and moderately (0.5 – 1 mm/day, ≈20%) in the winter. Their assessment also examined a evapotranspiration and runoff analysis and found that for Eastern North America, there is expected be little change in runoff, with most of the additional precipitation being lost via evapotranspiration.

However, GCMs are extremely computationally intense and by necessity coarse resolution simulations and are not suitable for regional or local scale hydrological modeling. Statistical downscaling of GCM results is the most common method for obtaining future climate projections to drive hydrological models (Werner & Cannon, 2015). Statistical downscaling involves identifying empirical relationships between GCM output and observed data, and using these relationships to create new climate models. Statistical downscaling can be used with observations from individual climate stations to

create local climate, or can be used with gridded observational data to produce climate data at a regional scale. Hydrological models run using statistically downscaled gridded data have been shown to produce stream flows that are statistically similar to observed flows (Salathé, 2005; Maurer et al, 2010; Werner & Cannon, 2015).

Maurer et al. (2010) reviewed three downscaling methods (BCSD, CA and BCCAQ) and found that the BCCAQ method consistently outperformed the others in three hydrologic measures for a large watershed in California. Werner & Cannon (2015) built upon their work by expanding the analysis to four additional methods and tested all seven against 28 metrics, focusing on extreme events for climate and hydrology for a large watershed in British Columbia. Their assessment found that the BCCAQ method passed the greatest number of hydrologic tests, while BCSD and BCSDX failed all tests related to winter low flow events.

2.2 Agent-Based Modeling

In addition to physical conditions and processes, hydrological systems can be strongly influenced by the actions of humans on the landscape. These processes can influence each other to create complex feedback effects, making modeling challenging. Integrating the hydrological model with other landscape process and management models in a multi-model platform allows for these feedbacks to be simulated. Agent-based modeling techniques, where numerous actors are programmed to make management decisions based on internal values and current landscape conditions, are well suited to assess possible futures for scenarios with complex and interdependent human effects (Bone et al., 2014).

Envision is "*a robust platform for integrating a variety of spatially explicit models of landscape change processes and production for conducting alternative futures analyses*" (Envision, 2015). Envision is designed with an extensible architecture that easily allows multiple models to be integrated and interact with each other. It also includes

> *a powerful 'multiagent modeling' subsystem that allows for the representation of human decision-makers in landscape simulations. Envision 'actors' make*

management decisions in parallel with landscape change models using a variety of decision models that can reflect actor values and incorporate landscape feedbacks" (Envision, 2015).

Envision has been used to assess the resiliency of the Williamette River Basin to water scarcity and climate change (Santelmann et al., 2012) and to assess socio-economic planning options for eastern Ontario that specifically consider the future of agriculture and climate change adaptation (Waldick, 2011).

The Flow framework is a standard Envision extension developed by the core Envision development team at the University of Oregon that powers most hydrological modelling capabilities of Envision. Flow provides a number of elements of hydrological process representation, including geometric representation of terrestrial and aquatic datasets used in the hydrologic model, topology, simulation control, data management, and default implementations of important hydrologic processes (Vache, 2015). Flow is highly flexible and can be configured to use existing or custom designed hydrological process models to calculate various hydrological fluxes, and also allows for user-defined fluxes (sources, sinks or transfers) at various stages of the hydrological model. HBV is one of the default models included with Flow.

2.3 Hydrological Modeling to Assess Climate Change Impacts

2.3.1 Classification of models

There is a wide diversity of models that have been developed to simulate hydrological processes in watersheds. Applications vary from assessing flow volumes for ecological minimum flows, identifying peak flood event flows for infrastructure design, identifying minimum drought flows for water extraction limiting, or calculating nutrient or sediment transport through a watershed. Each of these applications has different requirements. To help identify an appropriate model for use, hydrological models are generally classified based on three primary characteristics: spatial distribution, temporal distribution and model basis.

With respect to spatial distribution, models can be broadly classified as either lumped or distributed. Lumped models treat the entire watershed as a single spatial unit, and use parameter values that represent averages across the entire watershed (Kling & Gupta, 2009). Distributed models on the other hand subdivide the watershed into smaller pieces (possibly a grid) and can have different parameter values for each subunit (Beven, 1985). A middle ground "semi-distributed" distribution is also used in which watersheds are divided into a few subunits, but still use lumping at some scales or for some processes (Boyle et al., 2001).

Lumped models are simpler and require fewer input parameters, and are thus less computationally intense. They also can be useful in situations where little to no input data is available, as the number of parameter sets to calibrate is fewer and thus the number of potentially valid solutions is also reduced (Kling & Gupta, 2009). Distributed models on the other hand are better able to handle the varying conditions in most watersheds, and are thus more accurate – if sufficiently distributed, accurate input data is available (Carpenter & Georgakakos, 2006). However, a major review of distributed models by Reed et al (2004) found that more often than not, lumped models outperform distributed models, with a study by Kling & Gupta (2009) identifying calibration issues related to parameter complexity, identifiability and equifinality as major causes. Parameter identifiability is the concept of having a theoretical ideal parameter set, but not having sufficient measurements to identify it (Beven, 2001a), while equifinality is the concept of having numerous, diverse parameter sets which produce equally suitable results (Beven, 2001a).

In terms of temporal distribution, hydrological models are generally classified as either "continuous" or "event-based". Continuous models feature soil moisture accounting routines to keep track of water in the ground, and also account for losses over time from evapotranspiration and percolation (Beven, 2001b). Continuous models often have daily time-steps and are run over long continuous time spans of at least several years. Event-based models on the other hand are typically run over short durations of several hours or days and primarily used to predict peak flows. Event-based models typically

simplify soil moisture conditions as they generally are, or quickly become, uniform over these short duration events, and instead concentrate on accurately predicting water routing (Beven, 2001b).

The third characteristic is model basis, with models generally classified as empirical, conceptual or physically based. Broadly speaking, empirical models are defined by equations and parameters that are derived from statistical relationships between inputs and outputs with little to no reference to the laws of physics that govern hydrological processes (Aghakouchak & Habib, 2010). This is in direct contrast to physically based models which use parameters that are physical characteristics of materials and can therefore be measured, and link these together with detailed equations that describe the various physical processes that occur within the watershed such as conservation of mass and conservation of energy (Khakbaz et al., 2012). Conceptual models are also generally based on physical processes, but in this category, the underlying equations are simplified to expedite the calculations and reduce the amount of required input data (Khakbaz et al., 2012).

Empirical models are typical based on a small number of input variables, and thus can be operated simply, sometimes even graphically (e.g. SCS curve number). Conceptual models generally require calibration against observed data to determine the values of parameters for each watershed, a process that can be time and resource consuming and can also introduce uncertainty. However, this procedure means that conceptual models can be generalized in structure and are relatively scale independent, and thus the same model can be used at various scales by simply using/calibrating parameter values appropriate to the scale (Bergstrom & Graham, 1998). Physically based models however do not necessarily require calibration and can thus eliminate one significant source of potential error, as in the case with PROMET (Mauser & Bach, 2009).

Lumped conceptual models generally have fewer parameters and thus with fewer unknowns are less prone to equifinality, but may not have the required structure and resolution to properly simulate watershed processes (Martina, Todini & Liu, 2011). On the other hand, fully distributed conceptual models are particularly challenging to

calibrate as the number of parameter values are large, but the correlation between parameter values and physical characteristics is generally very weak, making measurement of parameters unreliable (Kling & Gupta, 2009). Even for physically-based, distributed models, the correlation of parameter values with physical characteristics of the materials and processes only holds at small spatial scales (Martina, Todini & Liu, 2011). This leads to the constraint that physically based models must also be highly spatially distributed to be useful. Both of these characteristics require additional input data and computational resources, thus the combination is particularly computationally taxing. Another consequence of this is that complex, physically based models do not necessarily produce better results than conceptual models due to uncertainty introduced with the required large amount of input data regarding the physical characteristics of the watershed at small scales (Blöschl & Montanari, 2010).

2.3.2 Review of models

Many different hydrological models have been developed and used to assess potential impacts of climate change. However, the selection of model can have a significant impact on the results (Velázquez et al., 2013), so it is important to choose a model that is appropriate for the study objectives.

The Soil Water Assessment Tool (SWAT) is a continuous, physically-based semi-distributed model that has been widely used to simulate watersheds around the world (Ahmad et al, 2011; Rahman et al, 2012; Sellami et al, 2016; Serpa et al., 2015). SWAT is suitable for simulating agricultural watersheds, and can be configured to simulate not only discharge but also other parameters such as nitrogen or sediment loads. However, SWAT is a complex, stand-alone model and is difficult to integrate with other models, making it unsuitable for use with Envision.

The Hydrologiska Byråns Vattenbalansavdelning (HBV) model (Bergström, 1976) is a conceptual rainfall-runoff model. Later derivatives (e.g. HBV-96, HBV-light) are semi-distributed spatially and operate on the concept of hydrological response units (HRUs) – discrete polygons that have uniform hydrological characteristics described by model parameters. HBV is typically operated on a daily time step and has routines for snow,

evapotranspiration, soil moisture, groundwater, and surface water routing. HBV has been successfully used in numerous studies in Canada and around the world (Kebede, Diekkrüger & Moges, 2014; Crossman et al, 2013; Samuel, Coulibaly & Metcalfe, 2012; Seibert & McDonnell, 2010) and has been previously used in conjunction with Envision (Inouye, 2014). Two important characteristics of HBV are its simplicity and its flexible structure that allows additional complexity to be added if justified by improved results (Lindström et al., 1997).

Other models such as WATFLOOD, Hydrotel and PROMET have been used to simulate impacts of climate change on hydrological systems. Like HBV, WATFLOOD is a conceptual hydrological model, but a comparison of WatFlood and HBV by Dibike & Coulibay (2007) found that HBV was better able to model flows in the Saguenay watershed of Quebec. Ludwig et al. (2009) used three different hydrological models to simulate the same watershed in Germany and found that the lumped conceptual model (HSAMI) did not produce acceptable results, while the other two (semi-distributed conceptual Hydrotel and physically based distributed PROMET) produced comparable results. This suggests that a semi-distributed conceptual model may be more appropriate as there was not sufficient improvement in results to justify the additional complexity and data requirements of the physically based, distributed PROMET.

For this work, a conceptual rainfall-runoff model based on HBV-light (Siebert & Vis, 2012) was used to calculate the vertical fluxes between hydrological layers, horizontal fluxes from catchments to stream reaches and water routing down the stream network.

2.3.3 Calibration and Validation of Hydrological Models

Hydrological models with empirical parameters, or physically-based parameters for which sufficient field data is unavailable, must be calibrated before use. Manual calibration requires significant experience and time, and often results in different parameter values being selected by different model operators (Zhang & Lindström, 1997). For these reasons, automatic calibration routines are generally preferred. Many automatic calibration routines exist, ranging from basic Monte Carlo scenarios using uniform parameter distributions, to complex evolutionary algorithms.

Seibert (1999) argued that Monte Carlo simulations are the most appropriate calibration method as their random nature removes any chance of bias related to the calibration algorithm. This approach has been found to work successfully in various studies around the world (Steele-Dunn et al, 2008; Zégre et al., 2010; Seibert & McDonnell, 2010). One advantage of the Monte Carlo simulation is that is generates a wide diversity of parameter sets which allows parameter uncertainty to be accounted for (Steel-Dunn et al., 2008).

For Monte Carlo simulations, parameter ranges and distributions must be specified. In situations where little is known about the potential values or distributions of parameters, sampling from a uniform distribution has been found to be effective (Zégre et al., 2010; Oni et al., 2014).

Another important consideration during model calibration is how to select the calibration dataset. Common practice in hydrological modeling is to use one continuous sequence of years as the calibration period, and an adjacent continuous sequence for validation. However, given climate variability, this approach can lead to an unrepresentative subset of data being selected for calibration. Addressing this, Moriasi et al. (2007) recommend ensuring that the calibration dataset contains a diversity of weather conditions including wet, dry and average precipitation years.

The duration of the calibration is also important, as insufficient data may not contain all normal conditions and processes, while too much data can waste computational resources and may average out any change in processes or characteristics of the watershed. A study by Yapo, Gupta & Sorooshian (1996) addressed this directly by assessing the number of years of data required to successfully calibrate thirteen parameters of a conceptual rainfall-runoff model. From their 344 calibrations using varying length periods selected from forty years of data, they conclude that eight years of calibration data are sufficient to produce a calibration that is relatively insensitive to the exact calibration period used. This result corresponds well with the work of Seibert & McDonnell (2010) who used an eight-year period to calibrate HBV and stated that

"*the rule of the thumb [is] that one needs 5–10 years of data to calibrate models like the HBV*" (Seibert & McDonnell, 2010).

The final major factor in model calibration is the selection of the evaluative function used to determine the skill of the simulation with respect to the observed data for each parameter set evaluated. To assess the overall suitability of each simulation, many studies combine several evaluative statistics into a single objective function (Lindström et al., 1997; Dakhlaoui, Bargaoui & Bárdossy, 2012; Inouye, 2014;). This allows runs to be compared and ranked by a single indicator in a qualitative and repeatable manner, while still incorporating results from a variety of assessments. Moriasi et al. (2007) emphasize the importance of using multiple statistics to assess the fit of the simulation. Commonly used evaluative measures include Nash-Sutcliffe Efficiency (NSE), the coefficient of determination (R^2) and Percent Bias (PBIAS).

NSE is a measure that compares the predictive capability of a simulation with the mean of the observations. NSE is widely used in hydrological modelling to assess the suitability of a model (Moriasi et al., 2007) and has been used in studies in Atlantic Canada (Ahmad et al, 2011; Roberts, Pryse-Phillips & Snelgrove, 2012). R^2 describes the proportion of the variance in measured data explained by the model, and has also been widely used. However, Moriasi et al. (2007) recommend against using R^2 as it is overly sensitive to extreme values and insensitive to additive and proportional differences.

NSE is also biased towards large flow event as it evaluates the square of the flow. However, using the NSE with the log transform of flow (NSE_{ln}) rather than the discharge itself has been found to be effective in reducing the effect of peak flows (Krause, Boyle & Bäse, 2005).

In addition to selecting the evaluative function, the acceptability threshold must also be considered. In addition to reviewing model evaluation statistics, Moriasi et al (2007) conducted an extensive review of literature using hydrological models and recorded the reported value of the evaluative function used and the authors analysis of model skill. Based on this dataset, they recommended that simulations can be considered

satisfactory if NSE > 0.50 and PBIAS < ±0.25 for models evaluated at a monthly time step.

2.3.4 Application of Hydrological Models in the Eastern North America Region

While there is very little published literature about the potential impact of climate change on the hydrological systems of Atlantic Canada, numerous studies have looked at various sites in eastern North America and give some indication of possible results.

Boyer et al. (2010) assessed the effect of climate change on stream flows in tributaries of the St. Lawrence River in Quebec using three GCMs and two emission scenarios from the IPCC's Fourth Assessment Report. Their simulations showed an increase in winter discharge and a decrease in spring discharge, which they link to higher mean temperatures and reduction of snow as a proportion of precipitation. These results correlate well with the work of Quilbé et al. (2008) from simulations of the nearby Chaudière River watershed using three GCMs and two emission scenarios. They reported a slight (5%) decrease in annual runoff, with a winter increase offset by decreases in other seasons. Closer to PEI, Rivard et al. (2014) used five climate scenarios to assess change in ground water recharge in the Annapolis Valley of neighbouring Nova Scotia, and found that by the 2050s, annual runoff decreased by 9 – 23%, with small increases in winter and major reductions in spring. They also observed that ET increased slightly (5 – 9%).

However, other studies have found contradicting results. Dibike and Coulibay (2005) compared results from two GCM downscaling methods and simulated the impact on hydrology of Quebec's Chute-du-Diable basin using two hydrological models, HBV and CEQUEAU. They found that both methods and models reported large increases in mean and peak flows during spring, small increases in the fall and large decreases in summer. They also noted that the differences observed between downscaling methods were larger than differences between hydrological models.

Roberts, Pryse-Phillips & Snelgrove (2012) modeled a sub-basin of the Lower Churchill River in Labrador and simulations for the 2050s found that the mean annual discharge

increased by 9%. Seasonally, their results showed increased winter flow but little change during the late summer and fall.

Tu (2009) assessed the impact of climate change and land use change on stream flows and nitrogen loads in several watersheds of eastern Massachusetts, and found that climate change had a larger effect on stream flows than land use change. His results showed small increases in annual discharge for most watersheds, but major redistribution of discharge across seasons, with increased discharge in the late fall and winter but reduced discharge in the remaining seasons, particularly the summer and early fall.

This review shows that there is no broad agreement on potential hydrological impacts of climate change in the eastern North America region. Location, selection of hydrological model and selection of climate scenario are all significant factors that influence results.

Chapter 3 Methodology

The methodology for this study is outlined in Figure 3.1 and detailed in the following sections.

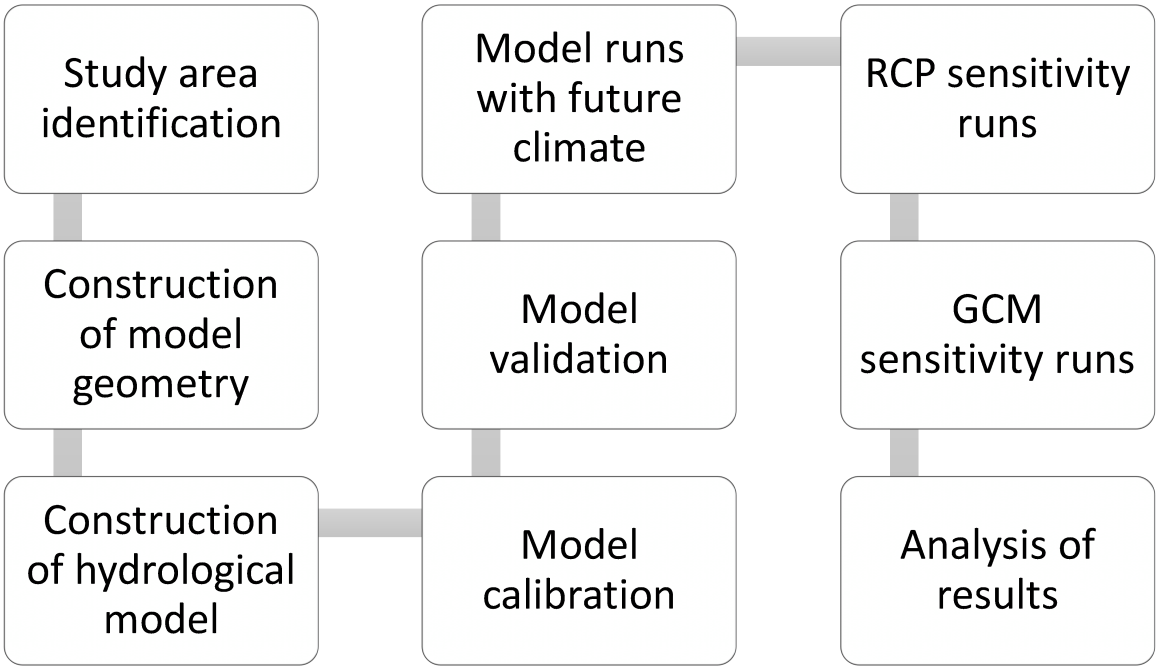

Figure 3.1- Flowchart for study methodology.

3.1 Study Area

The study area for this assessment consists of watersheds associated with five rivers in central and western PEI: Carruthers Brook, Dunk River, Wilmot River, West River and Winter River (Figure 3.2). These watersheds total 315 km^2 and contain the primary agricultural districts of PEI and provide municipal water to the cities of Charlottetown and Summerside. The region consists of flat plains and gently rolling hills. The highest point in the study area is 140 m at Springton in the northwest corner of the West River watershed, approximately 23 km from Charlottetown.

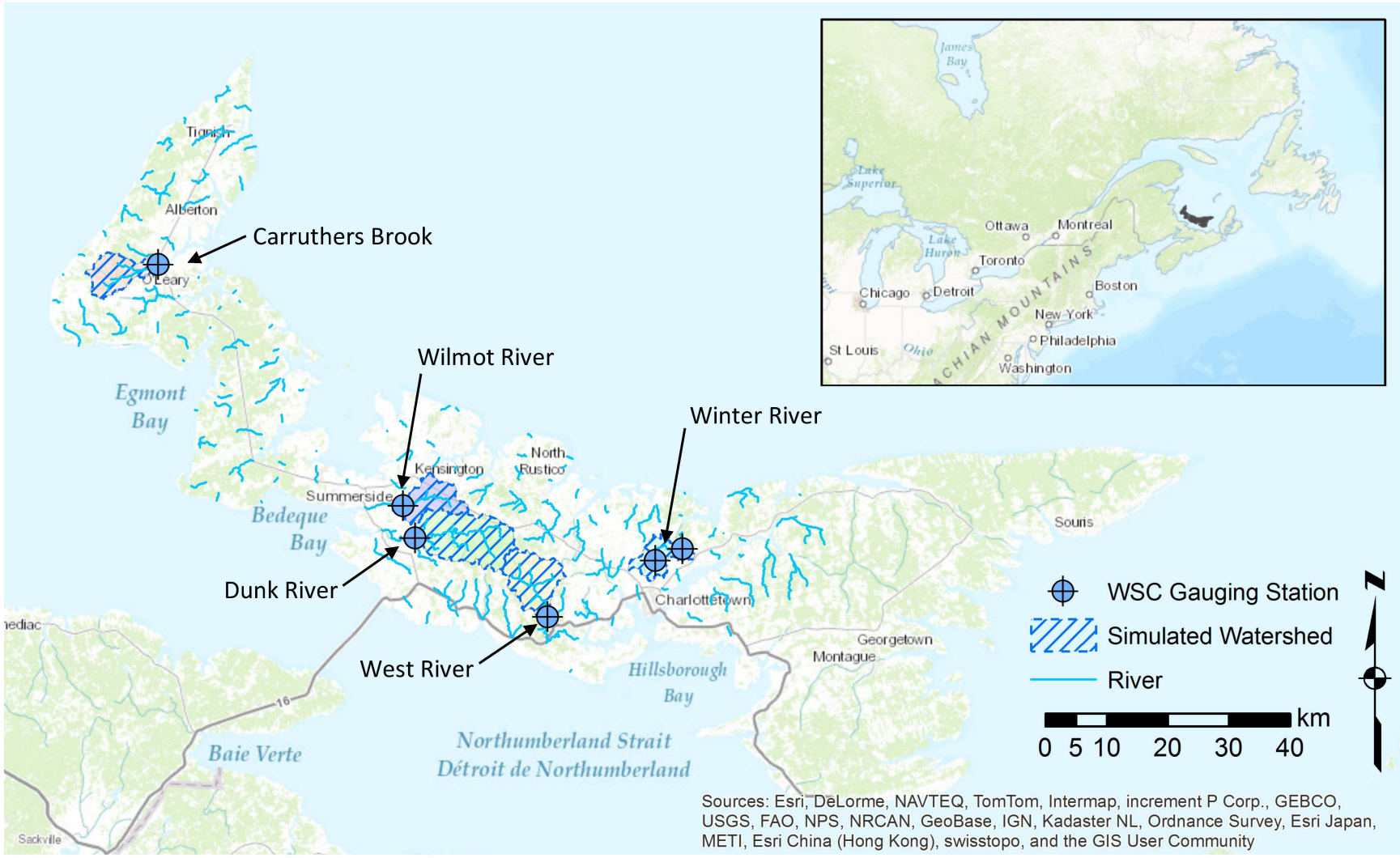

Figure 3.2 - Map of study area showing the five modeled watersheds.

3.1.1 Land Use/Land Cover (LULC)

Farmland is the dominant LULC for the study watersheds, with cultivated LULC accounting for approximately 31% of the total area and grasslands (hay, pasture and meadows) accounting for 23%. Forests are also well represented at 34%, while urban areas, wetlands, transportation and other account for the remainder of the study watersheds catchment area.

3.1.2 Climate

Environment and Climate Change Canada has been recording climate data at Charlottetown since 1910. For the period 1981 to 2010, the average annual temperature was 5.7 ˚C, with an average winter (DJF) temperature of -6.1 ˚C and an average summer (JJA) temperature of 17.2 ˚C. The annual precipitation was 1158 mm, with 290 cm of snow and 887 mm of rain. The average monthly climate data for this time period is shown in Figure 3.3.

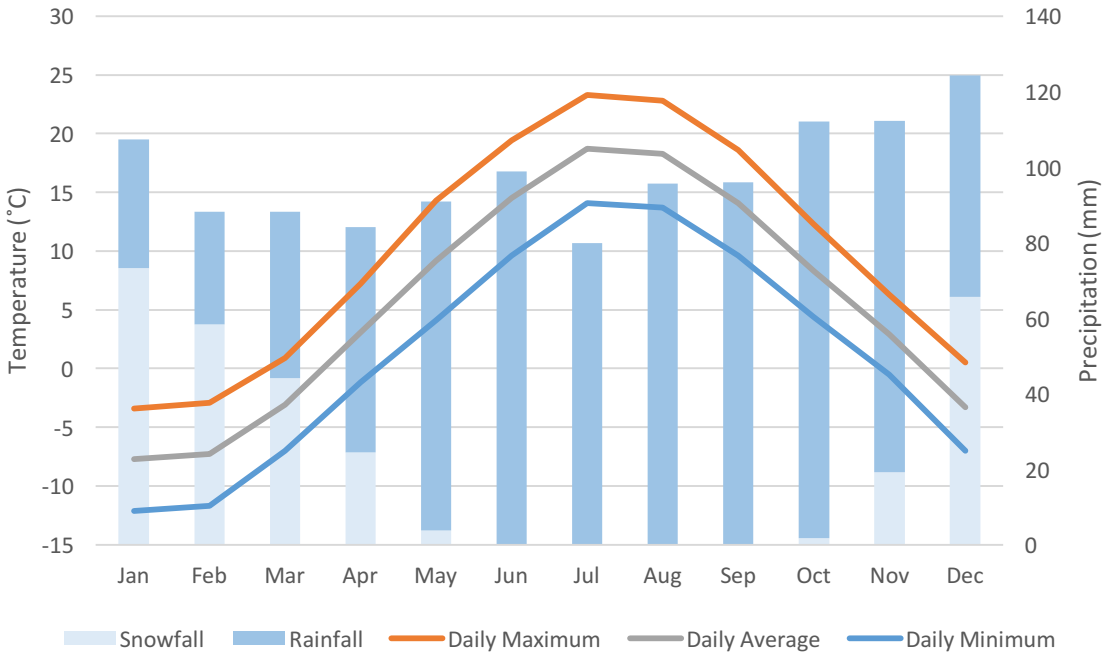

Figure 3.3 - 1981 to 2010 monthly climate normal data for Charlottetown.

3.1.3 Hydrology

The Water Survey of Canada (WSC) has at least one active gauging station in each of the five watersheds selected for analysis, with the Winter River watershed having two

gauging stations. Each station provides daily flow and level data. Table 1 summarizes the important information about the six stations. The daily Mean Annual Discharge for the six gauges ranges from 0.243 m^3/s to 2.577 m^3/s while the peak observed daily flow varies from 8.04 m^3/s to 63.1 m^3/s (Table 2). Figure 3.4 shows the annual hydrograph of mean daily flows for the 6 stations over the period of 1981 – 2014.

Table 1 - Details of Water Survey of Canada (WSC) Gauging Stations located in the study area.

WSC Station Number	Station Name	Station Location	Start Date	Drainage Area (km^2)
01CA003	Carruthers	Carruthers Brook near St. Anthony	24-Aug-1961	46.8
01CB002	Dunk	Dunk River at Wall Road	24-Aug-1961	114
01CB004	Wilmot	Wilmot River near Wilmot Valley	01-Jan-1972	45.4
01CC005	West	West River at Riverdale	21-Sep-1988	70.1
01CC002	Winter-L	Winter River near Suffolk	20-Oct-1967	37.5
01CC010	Winter-U	Winter River at Union	29-Jun-1992	16.8

Table 2 - Discharge characteristics for gauging stations for full years in the period 1981-2014.

Station Name	Drainage Area (km^2)	Mean Annual Drainage (m^3/s)	Peak Daily Discharge (m^3/s)
Carruthers	46.8	0.96	26.35
Dunk	114	2.58	63.10
Wilmot	45.4	0.94	35.50
West	70.1	1.79	45.14
Winter-L	37.5	0.66	14.52
Winter-U	16.8	0.24	8.04

Irrigation is very rare in PEI, reported at approximately 85 farms in the study area and accounting for less than 0.3% of the total cropland in 2011 (Statistics Canada, 2011).

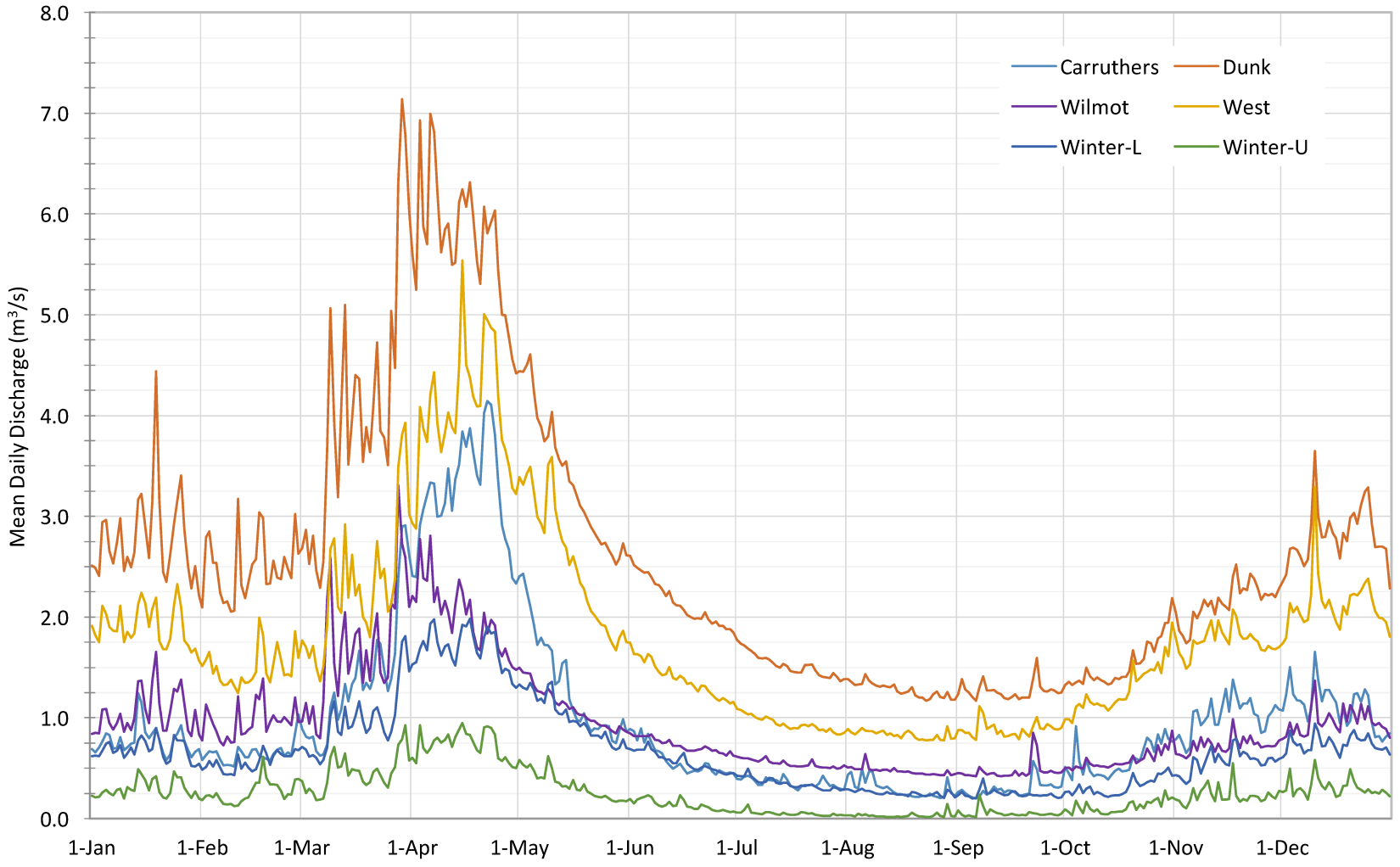

Figure 3.4 – Plot of mean daily flow over the period 1981 to 2014 for the six WSC gauging stations located within the study area.

3.2 Model Construction

3.2.1 Spatial Geometry

Input data is provided to Envision as a shapefile consisting of Integrated Decision Unit (IDU) polygons, where each IDU is treated as having homogeneous properties across its extent. The geometry of the IDUs is defined in the shapefile, and the metadata associated with each IDU is provided in the linked table with a column for each parameter. IDUs can be any shape or size, but all calculations are done at the IDU level and thus the finest spatial resolution for Envision calculations is set by IDU geometry.

For this study, three datasets were used to create the IDU geometry: landuse, cadastral and watershed boundaries. The landuse dataset was obtained from the PEI Department of Agriculture and Forestry, and was a vector polygon coverage developed from aerial photography flown across all of PEI in 2010. The cadastral data was obtained from the PEI Department of Finance and Municipal Affairs, and was also a vector polygon coverage of property boundaries, current as of 2014.

The Envision hydrological modelling framework requires specific metadata and relationships between the catchment areas being modeled and the associated stream network. For this reason, none of the available watershed boundary datasets were suitable and thus a new dataset had to be developed for this study. Catchment polygons and associated stream network lines for each study watershed were generated using the ArcHydro toolkit plugin for ArcGIS. The source digital elevation model (DEM) was created in ArcGIS at a 20 m grid resolution from 2 m interval contour lines provided by the PEI Department of Agriculture and Forestry. These contour lines were generated from a LiDAR survey of the entire island done in 2008.

To ensure spatial accuracy of the generated catchments and stream lines, stream lines from Natural Resource Canada's National Hydro Network dataset were burned into the generated DEM before catchment delineation. Given the size of the study watersheds, the daily time step of the hydrological model and available processing power, the

stream initiation threshold (drainage area at which a stream is formed) for catchment development was set at 5 km^2.

The three input datasets were unioned together in ArcGIS to create the IDU polygons. Envision developers recommend limiting the IDU dataset to approximately 100,000 polygons, and therefore the IDU coverage was processed to merge the smallest IDUs into adjacent IDUs until this was achieved. During this merging, catchment boundaries were strictly maintained. The resulting IDU coverage contains 104,944 IDUs with a median size of 2.3 ha and 99% of polygons ranging between 0.1 ha and 20 ha.

3.3 Hydrological Model

Following from HBV-light, the hydrological model defines five layers for each HRU: snow (HRU_{snow}), snowmelt (HRU_{melt}), vegetation (HRU_{veg}), upper groundwater zone (HRU_{UZ}) and lower groundwater zone (HRU_{LZ}). The model operates at a daily time-step, with the state of each layer being calculated once each day. The operation of the model is specified by thirteen parameters which are summarized in Table 3 and detailed in the following sections which describe how the various hydrological processes are handled by the model.

Table 3 - Parameters for hydrological model.

Parameter	Description	Units
TT	Threshold temperate that separates rain from snow	˚C
CFMAX	Degree day factor controlling the melting of snow	mm/(˚C day)
SFCF	Snowfall correction factor	-
CWH	Water holding capacity of snowpack	-
CFR	Snowmelt refreezing factor	-
FC	Maximum soil moisture content	mm
WP	Wilting point – minimum water in HRU_{veg} layer for ET to occur	mm
BETA	Infiltration shape coefficient	-
PERC	Percolation coefficient	day^{-1}
UZL	Peak response threshold	mm
K0	Peak response recession coefficient	day^{-1}
K1	Fast response recession coefficient	day^{-1}
K2	Slow response recession coefficient	day^{-1}

3.3.1 Precipitation, Snow Accumulation and Snow Melt

The threshold temperature parameter (TT) divides precipitation into rain (RF) and snow (SF), with rainfall occurring when the mean daily temperature (*T(t)*) is above TT and snowfall occurring below.

Snow accumulates in the HRU_{snow} layer after the snowfall correction factor (SFCF) is applied to account for snowfall processes not explicitly modeled (e.g. snowfall data errors, sublimation). When the mean daily temperature rises above TT, snow in the HRU_{snow} layer starts to melt based on a degree-day parameter CFMAX producing meltwater (M) which accumulates in the HRU_{melt} layer (Eq. 1). Any rain that falls on snow is also stored in the HRU_{melt} layer.

$$M = CFMAX \cdot (T(t) - TT) \quad (1)$$

The water holding capacity of snowpack (CWH) parameter sets the maximum proportion of meltwater that can be retained as a proportion to the amount of snow. Rainfall and snowmelt above this proportion are passed to the infiltration routine.

When the mean daily temperature drops below TT, meltwater begins to refreeze. Refreezing (REFR) is calculated similarly to melting but with the addition of a snowmelt refreezing factor (CRF) parameter (Eq. 2)

$$\mathrm{REFR} = \mathrm{CFR} \cdot \mathrm{CFMAX} \cdot (\mathrm{T(t)} - \mathrm{TT}) \quad (2)$$

3.3.2 Infiltration

Rainfall and snowmelt beyond the water holding capacity of snowpack are passed to the infiltration routine and divided into recharge (R) to groundwater (HRU_{UZ} layer) and infiltration (I) to soil (HRU_{veg} layer). Recharge is a function of the ratio of current soil moisture (SM(t)) to the maximum soil moisture (FC) parameter modified by the infiltration shape coefficient (BETA) parameter (Eq. 3). Infiltration is the difference between the input and recharge.

$$R = \left(\frac{SM(t)}{FC}\right)^{BETA} \quad (3)$$

3.3.3 Evapotranspiration

Like HBV, the model handles evapotranspiration (ET) by first calculating a potential evapotranspiration (PET) which represents the evapotranspiration that would occur in unlimited soil moisture conditions.

PET is calculated using the Baier-Robertson method (Baier & Robinson, 1965). The Baier-Robertson method is widely used across Canada (Bootsma, 1994; Almorox, Quej & Martí, 2015; Kersebaum et al, 2008) and requires only maximum and minimum temperature as input climate data which makes it suitable for use with downscaled future climate data.

To calculate the actual ET (AET) and account for water limitations, the PET value is then modified based on the current soil moisture (amount of water in HRU_{veg} layer) and the wilting point (WP) parameter. When soil moisture is less than WP, ET is set to zero, while when soil moisture is greater than the wet threshold ($0.5 \cdot$ (FC-WP)) , AET is set to PET. Between WP and the threshold, ET is a linear function ranging between zero and PET. The AET is removed from the HRU_{veg} layer.

3.3.4 Percolation and Runoff

Recharge from the infiltration routine is added to the upper groundwater (HRU_{UZ} layer). Percolation (PC) from upper to lower groundwater (HRU_{UZ} layer to the HRU_{LZ} layer) is calculated by multiplying the water content of the upper groundwater (UZ(t)) by the percolation coefficient (PERC).

Runoff from the HRU to the stream is taken from the two groundwater layers and calculated using three distinct response recession coefficient (K0, K1 and K2) parameters. The peak response (Q0 – Eq. 4) and fast response (Q1 – Eq. 5) runoff fluxes are taken from the upper groundwater layer, with the peak response only occurring when the water content of the upper groundwater is above the peak response

threshold (UZL) parameter. The slow response (Q2) runoff flux is taken from the lower groundwater layer based on the water content of the lower groundwater (LZ(t)) (Eq 6).

$$Q0 = K0 \cdot \max(UZ(t) - ULZ, 0) \quad (4)$$

$$Q1 = K1 \cdot UZ(t) \quad 0 \leq UZ(t) \leq UZL \quad (5)$$

$$Q2 = K2 \cdot LZ(t) \quad (6)$$

3.3.5 Stream Routing

Once runoff is generated from an HRU, it is added to the stream reach associated with the HRU's catchment, and from there is routed down the stream network to the ocean. The routing routine is where this conceptual rainfall-runoff model diverges from HBV-light. For the routing function, this model uses a kinematic wave analog and is solved according to the implicit kinematic wave solution of Chow, Maidment, and Mays (1988). Two parameters, width to depth ratio (W:D) and Manning's roughness coefficient (*n*), are required to parameterize the routing model. A sensitivity analysis for two watersheds (Dunk River and West River) found that neither parameter had a large impact on simulated flows, and thus values were selected based on catchment characteristics. The width to depth ratio was set at 10 which conforms with the average calculated by Fecko & Johnson (2008) for the Eastern US Coastal Plain physiographic region. Manning's number was set to 0.03 following Chow (1959).

3.3.6 Initial Conditions

Initial conditions (volume of water in each of the five model layers) for the hydrological model were not known and therefore had to be assumed. This leads to inaccurate flow simulations at the start of the model. To prevent these inaccurate flows from affecting the simulation, a model warm-up period was introduced, during which the model ran normally but the results were ignored, allowing the system to stabilize. To determine an appropriate warm-up period, the model was run twice with different start dates (1-Jan-1995 and 1-Jan-2002). For all five gauged watersheds, the two simulations were found to consistently produce equal flow values to four significant figures over five

consecutive days starting in the fourth year. Based on this result, the warm-up period was set at four years.

3.4 Model Calibration

To calibrate the hydrological model, an initial screening was conducted by running 2000 simulations for the period 1995 through 2014 using observed weather data recorded at Charlottetown. The screening runs were conducted in three parallel batches to better utilize processing resources. The details of the screening runs are shown in Table 4.

Table 4 - Screening run details.

Batch	# of Runs	Run Numbers
1	600	1000-1599
2	700	2000-2699
3	700	3000-3699

To create a calibration dataset that contains a diversity of weather conditions including wet, dry and average precipitation years as recommended by Moriasi et al. (2007), the total annual precipitation was calculated for each year between 1995 and 2000 and years were assigned to each period (calibration and validation) to ensure a mix of climatic conditions.

Each simulation used a unique set of values for the model parameters. Two of the parameters, CFR and CWH, were held constant at 0.05 and 0.1 respectively while the eleven remaining parameters were assigned a value randomly selected from a specified range using a uniform distribution. The ranges used during model calibration for each parameter are shown in Table 5. Initial ranges were taken from Seibert (1999) and Abebe, Ogden & Pradhan (2010), and were expanded whenever best fit simulations from several preliminary calibration runs had parameter values near a maximum or minimum limit.

Table 5 - Ranges used for parameter selection during model calibration.

HBV Parameter	Minimum Value	Maximum Value
TT	-2	2
CFMAX	1	10
SFCF	0.5	1.5
FC	50	500
BETA	1	6
PERC	0	3
UZL	0	100
K0	0.05	0.5
K1	0.01	0.4
K2	0.001	0.15
WP	1	25

For each run, the simulated flows were compared with the observed flow records from the six WSC gauging stations located within the study area, and three metrics were calculated to determine the fit of the simulation: Nash-Sutcliffe Efficiency (NSE) for daily flows (NSE_d), NSE for log-transform (NSE_{ln}) of daily flows (NSE_l_d) and Percent Bias (PBIAS).

The NSE (Eq. 7) compares the predictive capability of a simulation with the mean of the observations, with possible values ranging from 1 to -∞. An NSE value of 1 indicates that the simulation is a perfect fit for the observations, while a value of 0 means that the observation mean is equally predictive compared to the simulation. Any value less than 0 indicates that the observation mean is a better fit than the simulation.

$$NSE(t) = 1 - \frac{\sum(Q_{obs}(t) - Q_{sim}(t))^2}{\sum(Q_{obs}(t) - \bar{Q}_{obs}(t))^2} \quad (7)$$

Given its use of the square of flow, the NSE metric is biased towards high flow periods. The NSE_{ln} has been shown to be less sensitive to these peak flows, and was used to better assess fit of mean and low-flow periods. NSE_{ln} is calculated by passing the logarithm of flow to the NSE function (Eq. 7) rather than the raw flow value.

PBIAS (Eq. 8) is a volumetric error measure that identifies consistent over- or under-prediction of the simulation.

$$PBIAS = \frac{\sum(Q_{sim} - Q_{obs})}{\sum Q_{obs}} \quad (8)$$

These three statistics were combined into a single objective function (OBJ) (Eq. 9) which was used to evaluate model performance. This objective function extends the practice of reducing the NSE value by the magnitude of the PBIAS measure, as done by Lindström et al (1997), to also include the NSE_{ln}. The weighting factor for the PBIAS measure, *w*, was taken to be 0.1 as recommended by Lindström et al (1997).

$$OBJ = \frac{NSE\_d \ + \ NSE\_l\_d - w \cdot |PBIAS|}{2} \quad (9)$$

From the screening run, the top fifty parameter sets by the objective function for the calibration period (Obj_c) were identified for each watershed. Each identified run was assigned a rank between 50 and 1 in descending order, with the best run in each watershed being 50 and the 50th best run being 1. To identify parameter sets that performed well across all study watersheds, the simulations were then sorted by run number and the six rank values were summed to create a SA_Rank value. The top ten model runs by SA_Rank were then carried forward for model validation.

The results of the calibration were validated using the temporal validation technique. In this technique, the model is run on data from a different time-period and the same model statistics (NSE_d, NSE_l_D and PBIAS) are calculated to verify that model performance is satisfactory for periods outside of the calibration period. Spatial validation was also considered for this study but was found to be impractical given the limited number of streamflow gauges and the large distances between some of the gauged watersheds.

3.5 Future Climate Data Screening Assessment

In order to assess the impact of climate change on future stream flows in the study area, future local climate simulation data is required to drive the hydrological model. Gridded climate data covering the study area statistically downscaled from GCMs using the BCCAQ method was obtained from the Pacific Climate Impacts Consortium (Pacific Climate Impacts Consortium, 2014). To identify what GCM to use, the performance of GCMs in simulating past climate was assessed.

Sheffield et al. (2013) evaluated the historical performance of seventeen core CMIP5 models in North America, and based on this assessment, four of the top performing GCMs were selected to examine modelling skill specifically in the study area:

- GFDL-ESM2G, developed by National Oceanic and Atmospheric Administration Geophysical Fluid Dynamics Laboratory in the United States (Donner et al., 2011);
- MRI-CGCM3, developed by the Meteorological Research Institute, Japan (Yukimoto et al., 2012);
- CNRM-CM5, developed by the National Centre for Meteorological Research, France (Voldoire et al., 2013); and
- MIROC5, developed in Japan by the University of Tokyo, National Institute for Environmental Studies and the Japan Agency for Marine-Earth Science and Technology (Watanabe et al., 2010).

Hindcast data from these four models were then compared to observation data at Charlottetown for the historical period 1980-2005 and the GCM with the best fit to the observed record was selected for use as the climate inputs in future modeling.

3.6 Emission Scenario and GCM Sensitivity Assessments

To assess the full spectrum of possible future climate scenarios with respect to anthropogenic climate impacts, downscaled climate data from three emission scenarios (RCP2.6, RCP4.5 and RCP8.5) for the best performing GCM were selected for use as input to the hydrological model.

Although one GCM was selected for use in future modelling, uncertainty associated with climate change means it important to not rely solely on one GCM (Chen et al, 2010, Werner & Cannon, 2015). Therefore, a GCM sensitivity analysis was conducted by using statistically downscaled climate data for the three other GCMs as input to the calibrated hydrological model and assessing the results. To simplify the assessment, only the RCP8.5 emissions scenario was used for the GCM sensitivity analysis.

3.7 Drought Assessment

Given recent concerns about inadequate stream flows in PEI rivers during summer low flow periods, assessing future low-flow rates is particularly relevant for the study area. There are numerous indicators that are used to assess low-flow periods, with 7Q10 and 60Q50 being two of the commonly used. These indicators in X-Q-Y format represent the mean flow over a period of X days that would be expected to occur once in Y years, thus 7Q10 is the minimum 7-day mean flow that is expected once in 10 years, while the 60Q50 is the minimum 60-day mean flow that is expected once in 50 years.

To calculate these indicators, the daily flow outputs from the observed and simulated records were assessed and the minimum 7 and 60-day mean flow was identified for each year. To better target minimum summer low-flow periods, a hydrological year of 1-Apr to 31-Mar was used, and the mean flows were calculated using trailing windows with end dates restricted to between 1-May and 1-Nov.

Given that the stream gauge for West River was only installed in 1988, a 25-year sample (1990-2014) was collected to assess droughts in the historic period, while a larger 30-year sample (2015-2044) was used for the future simulations to reduce error. The sample data was then fit to both the three parameter Weibull and General Extreme Value (GEV) distributions using EasyFit version 5.6 software. As recommended by Nathan & McMahon (1990), only data points with an exceedance value of greater than 80% were used in the fitting procedure to account for annual minimums that do not represent actual drought conditions. The Kolmogorov-Smirnov goodness-of-fit measure

(K-S) was used to select the best fitting distribution for each dataset, and the selected distribution was used to calculate the magnitude of the desired return period event.

Chapter 4 Results and Discussion

4.1 Model Calibration

To select an appropriate calibration period containing a diversity of climatic conditions, the annual precipitation was calculated for each year in the initial simulation period (Table 6). Given that dry years are clustered early in the period and wet years are clustered late, years were alternatingly assigned to calibration/validation. This results in an appropriate mix of conditions in both periods, and creates a better balance than two sequential periods. This alternating classification system may also help address any systematic changes in climate or watershed processes by calibrating to a wider temporal span.

Table 6 - Calibration and validation period selection. Years were classified as "Wet", "Average" or "Dry" by annual precipitation being in the top, middle or bottom third of the sample.

Year	Annual Precipitation (mm)	Classification	Role Assigned
1995	937		Warm-up
1996	1209		Warm-up
1997	848		Warm-up
1998	1140		Warm-up
1999	901	Dry	Calibration
2000	1098	Average	Validation
2001	787	Dry	Calibration
2002	1297	Average	Validation
2003	1024	Dry	Calibration
2004	987	Dry	Validation
2005	1116	Average	Calibration
2006	1134	Average	Validation
2007	1102	Average	Calibration
2008	1494	Wet	Validation
2009	1428	Wet	Calibration
2010	1354	Wet	Validation
2011	1370	Wet	Calibration
2012	1086	Dry	Validation
2013	1159	Average	Calibration
2014	1454	Wet	Validation

From the two thousand runs conducted in the model screening phase, the top twenty runs sorted by the value of the objective function over the calibration period (Obj_c)

were extracted for each watershed. Table 7 shows these results for all six watersheds sorted by SA_Rank.

Table 7 – Top twenty simulations across the study area. Rank values for each watershed are based on the Obj_c evaluative function, and the combined results are ordered by SA_Rank. The top ten simulations for each watershed are highlighted.

Run #	Dunk	Wilmot	West	Carruthers	Winter -L	Winter-U	SA_Rank	Sites
2228	**50**	**50**	**50**	**42**	**49**	-	241	5
1571	**48**	**48**	**46**	37	**45**	-	224	5
3488	**47**	**46**	**45**	**43**	34	-	215	5
2091	**42**	**42**	**43**	**49**	38	-	214	5
1139	**44**	**44**	**44**	**44**	27	-	203	5
1289	37	37	40	**50**	39	-	203	5
2154	**41**	**43**	39	38	**41**	-	202	5
1376	**49**	**49**	**47**	8	**47**	-	200	5
2678	39	39	38	**45**	37	-	198	5
3162	**46**	38	**49**	-	**48**	-	181	4
2179	**45**	**47**	**42**	2	**44**	-	180	5
2457	**43**	34	**48**	-	**50**	-	175	4
3170	40	**45**	32	13	40	-	170	5
1144	32	33	31	**46**	24	23	166	6
3221	38	40	37	7	31	-	153	5
2687	36	35	**41**	18	19	-	149	5
2201	34	36	35	27	9	-	141	5
2090	18	16	21	40	36	-	131	5
1147	19	21	20	**47**	21	-	128	5
2039	28	26	36	21	16	-	127	5

This data shows that in general, all of the high performing parameter sets give good results in multiple watersheds, with 31 top-ten results for individual watersheds contained in the top twenty runs. This suggests that the gauged watersheds behave similarly in the hydrological model, and thus it may be appropriate to use a single parameter set to operate on all watersheds rather than individual parameter sets for each watershed. Not all watersheds are equally represented however, as Winter Upper has only one top 50 run in the top 20 overall.

While rank is a useful way to identify high-performing parameter sets given varying model performance in different watersheds, the final selection of parameter sets was done by assessing objective function values for the calibration period. Table 8 presents

values for NSE, NSE_{ln}, PBIAS and OBJ for each of the top ten parameter sets in the calibration period, selected by SA_Rank. These results show that the top ten runs by SA_Rank contain the best performing run for four of the six watersheds, while a fifth, the Winter-L watershed, has five of its top ten runs in the top ten regional runs. Based on this, these regional top ten runs were deemed representative of best model performance and were carried forward for validation.

Overall, the simulations perform best for West River, Dunk River and Winter Lower, with Carruthers Brook and Wilmot River giving lower values. Performance of the top ten simulations in the Winter Upper watershed is very poor. In most cases, NSE_{ln} values are significantly greater than NSE values, suggesting that the model is better at predicting low flow periods which typically occur during the summer months.

PBIAS values for Winter-L and Winter-U are consistently large and of uniform sign, averaging -0.406 for Winter-L and +0.400 for Winter-U. These magnitudes are both well above the ±0.25 acceptable value recommended by Moriasi et al. (2007) and suggest that there are processes occurring in this watershed that are not being accounted for by the model.

One unique process related to the Winter River watershed is the extraction of groundwater for the City of Charlottetown, which obtains all its municipal water from three well fields located in the Winter River catchment. Two well fields are located in the Winter-U catchment and the third in the Winter-L catchment, and together the average daily extraction was approximately 19,500 m^3 in 2014. However, treated effluent from the municipal waste water treatment plant is discharged into Charlottetown Harbour, thus piping water out of the Winter River watershed and potentially explaining why the hydrological model simulations consistently over-predict flows in the Winter-U watershed. Attempts to incorporate this groundwater extraction into the hydrological model were unsuccessful, as extraction rates are higher than local infiltration and HBV does not account for groundwater flow between catchments, leading to negative water volumes in the groundwater layers for the Winter-U catchment.

Table 8 - NSE, NSE_{ln}, PBIAS and OBJ values from the calibration period for the top ten parameter sets by SA_Rank. The "Max" value is the maximum from all 2000 simulations.

	Dunk				Wilmot				West			
Max	*0.224*	*0.449*		*0.323*	*0.135*	*0.294*		*0.172*	*0.304*	*0.485*		*0.373*
Run #	**NSE_d_c**	**NSE_l_c**	**PBIAS_d_c**	**Obj_c**	**NSE_d_c**	**NSE_l_c**	**PBIAS_d_c**	**Obj_c**	**NSE_d_c**	**NSE_l_c**	**PBIAS_d_c**	**Obj_c**
2228	0.207	0.449	-0.096	**0.323**	0.051	0.294	-0.021	**0.172**	0.292	0.473	-0.186	**0.373**
1571	0.132	0.363	-0.184	**0.239**	0.012	0.255	-0.117	**0.128**	0.208	0.350	-0.265	**0.266**
3488	0.163	0.222	-0.202	**0.182**	0.031	0.117	-0.135	**0.067**	0.274	0.282	-0.281	**0.264**
2091	0.130	0.072	-0.124	**0.095**	0.018	-0.033	-0.052	**-0.010**	0.240	0.208	-0.212	**0.213**
1139	0.189	0.086	-0.192	**0.128**	0.036	-0.019	-0.125	**0.002**	0.304	0.186	-0.273	**0.231**
1289	0.041	0.029	-0.112	**0.029**	-0.109	-0.076	-0.038	**-0.095**	0.158	0.117	-0.200	**0.127**
2154	-0.048	0.240	-0.129	**0.090**	-0.153	0.153	-0.057	**-0.003**	0.026	0.237	-0.216	**0.121**
1376	0.087	0.426	-0.086	**0.252**	0.024	0.281	-0.011	**0.152**	0.152	0.449	-0.177	**0.292**
2678	0.089	0.066	-0.162	**0.069**	-0.018	-0.027	-0.093	**-0.027**	0.139	0.119	-0.245	**0.117**
3162	0.062	0.254	0.135	**0.151**	-0.074	0.010	0.230	**-0.044**	0.224	0.423	0.022	**0.322**

	Carruthers				Winter-L				Winter-U			
Max	*0.339*	*0.472*		*0.367*	*0.337*	*0.473*		*0.335*	*0.252*	*0.382*		*0.279*
Run #	**NSE_d_c**	**NSE_l_c**	**PBIAS_d_c**	**Obj_c**	**NSE_d_c**	**NSE_l_c**	**PBIAS_d_c**	**Obj_c**	**NSE_d_c**	**NSE_l_c**	**PBIAS_d_c**	**Obj_c**
2228	0.269	0.329	0.006	**0.299**	0.233	0.473	-0.372	**0.335**	0.128	-0.234	0.482	**-0.077**
1571	0.252	0.330	-0.091	**0.286**	0.187	0.255	-0.433	**0.199**	0.116	-0.218	0.336	**-0.068**
3488	0.227	0.386	-0.111	**0.301**	0.137	0.204	-0.445	**0.149**	0.120	-0.194	0.307	**-0.052**
2091	0.268	0.399	-0.025	**0.332**	0.246	0.122	-0.392	**0.164**	0.092	-0.164	0.433	**-0.057**
1139	0.287	0.333	-0.100	**0.305**	0.166	0.078	-0.439	**0.100**	0.124	-0.247	0.323	**-0.078**
1289	0.263	0.472	-0.011	**0.367**	0.242	0.131	-0.383	**0.167**	-0.067	-0.042	0.454	**-0.077**
2154	0.179	0.397	-0.030	**0.287**	0.197	0.196	-0.395	**0.177**	-0.103	-0.178	0.426	**-0.162**
1376	0.140	0.283	0.018	**0.211**	0.128	0.391	-0.366	**0.241**	0.001	-0.283	0.494	**-0.166**
2678	0.250	0.370	-0.067	**0.307**	0.252	0.111	-0.418	**0.160**	0.071	-0.131	0.371	**-0.049**
3162	0.207	0.180	0.265	**0.180**	0.269	0.418	-0.211	**0.333**	-0.092	-0.417	0.862	**-0.298**

Due to the consistently large PBIAS values and low OBJ values, the Winter-U gauge was removed from further analysis. The Winter-L gauge also showed poor PBIAS results in nine of the regional top ten parameter sets, however examination of the top twenty parameter sets for the individual watershed shows that simulations with acceptable OBJ and PBIAS values are present, as shown in Table 9. This suggests that the model is capable of producing acceptable simulations for the Winter-L gauge, however the characteristics of the watershed are different than the other gauged watersheds and are better modelled with a distinct parameter set. Two of these top twenty runs with acceptable PBIAS values from Winter-L (2457 and 3162) were carried forward to validation.

Table 9 - Top ten model calibration runs for Winter-L by OBJ where |PBIAS| < 0.25. Runs carried forward for validation are indicated in bold.

Max	*0.337*	*0.473*		*0.335*
Run #	**NSE_d_c**	**NSE_l_c**	**PBIAS_d_c**	**Obj_c**
2457	**0.223**	**0.466**	**-0.184**	**0.335**
3162	**0.269**	**0.418**	**-0.211**	**0.333**
1196	0.171	0.211	-0.193	0.181
1593	0.294	-0.014	-0.212	0.130
2652	0.227	0.036	-0.127	0.125
3061	0.115	0.098	-0.094	0.102
2093	0.086	0.015	-0.155	0.043
2153	0.132	-0.185	-0.223	-0.038
2056	0.155	-0.247	-0.244	-0.058
1276	0.197	-0.318	-0.190	-0.070

4.2 Model Validation

The top ten parameter sets for the study area plus two high performing parameter sets for the Winter-L watershed were assessed in the model validation phase. The results of the validation are shown in Table 10.

Table 10 - OBJ values during the calibration and validation periods for twelve runs selected for validation.

	Dunk		Wilmot		West		Carruthers		Winter-L			
Max	*0.323*	*0.154*	*0.172*	*0.036*	*0.373*	*0.296*	*0.367*	*0.322*	*0.335*	*0.355*		
Run #	**Obj_c**	**Obj_v**	**Obj_c**	**Obj_v**	**Obj_c**	**Obj_v**	**Obj_c**	**Obj_v**	**Obj_c**	**Obj_v**	**Mean**	**Mean Change**
2228	0.323	0.147	0.172	-0.021	0.373	0.296	0.299	0.234	-	-	**0.228**	-0.128
1571	0.239	-0.004	0.128	-0.111	0.266	0.146	0.286	0.279	-	-	0.154	-0.152
3488	0.182	0.022	0.067	-0.116	0.264	0.129	0.301	0.208	-	-	0.132	-0.143
2091	0.095	-0.171	-0.010	-0.327	0.213	0.071	0.332	0.240	-	-	0.055	-0.204
1139	0.128	-0.073	0.002	-0.224	0.231	0.064	0.305	0.220	-	-	0.082	-0.170
1289	0.029	-0.443	-0.095	-0.601	0.127	-0.129	0.367	0.239	-	-	-0.063	-0.340
2154	0.090	-0.144	-0.003	-0.283	0.121	0.074	0.287	0.268	-	-	0.051	-0.145
1376	0.252	0.132	0.152	-0.024	0.292	0.242	0.211	0.102	-	-	0.170	-0.114
2678	0.069	-0.253	-0.027	-0.369	0.117	-0.061	0.307	0.253	-	-	0.004	-0.224
3162	0.151	-0.070	-0.044	-0.345	0.322	0.275	0.180	0.075	-	-	0.068	-0.169
2457	-	-	-	-	-	-	-	-	0.335	0.170	0.252	-0.165
3162	-	-	-	-	-	-	-	-	0.333	0.355	**0.344**	0.022

Run 2228 has the best average OBJ value and also had among the lowest decrease in the validation period, and so was selected as the primary parameter set for future modelling. Run 3162 performed better in the validation than its alternate for Winter-L and thus was selected for use in final modelling in that watershed.

Figures Figure 4.1 to Figure 4.3 show daily simulated flow compared to observed flows for West River and Carruthers Brook in three hydrological years (Oct – Sep in 2004/05, 2000/01 and 2010/11), representative of average, dry and wet years. Precipitation recorded at Charlottetown (used for all watersheds during calibration) is also shown. These results show the range of model skill across watersheds and climatic conditions. In general, the simulations fit well with observed flows during the summer low flow period (June- Oct). Winter flow events are generally timed well in the simulations, but are usually smoothed out over a longer period. Spring melt peak flows are generally below observed values, except in situations where abnormal warm periods cause significant premature melting of the snow pack (as in 2002).

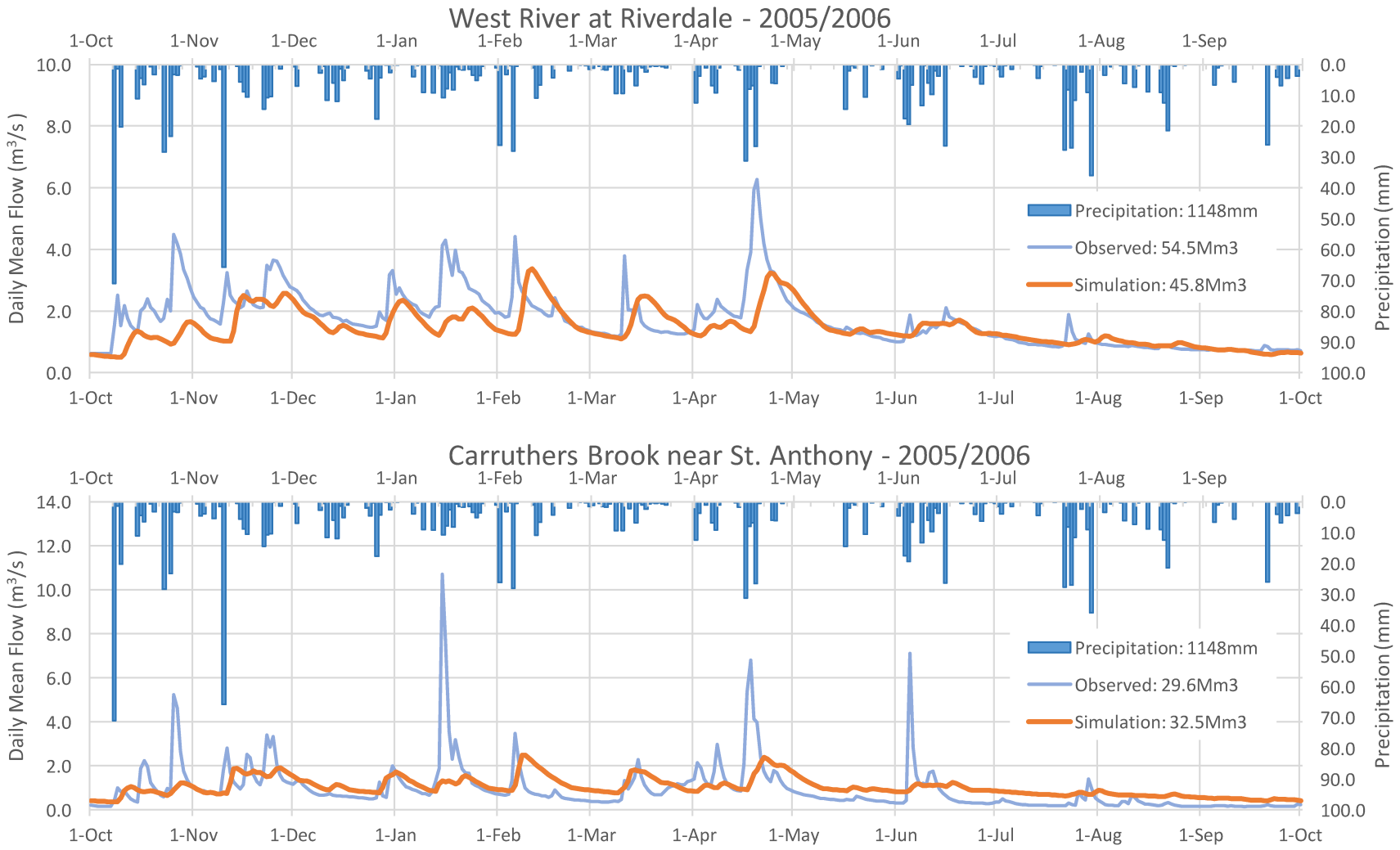

Figure 4.1 - Simulated vs observed flows for West River and Carruthers Brook for 2005/06 (average year). The simulations for both watersheds produce satisfactory results for summer low-flow periods but misses winter peak flows.

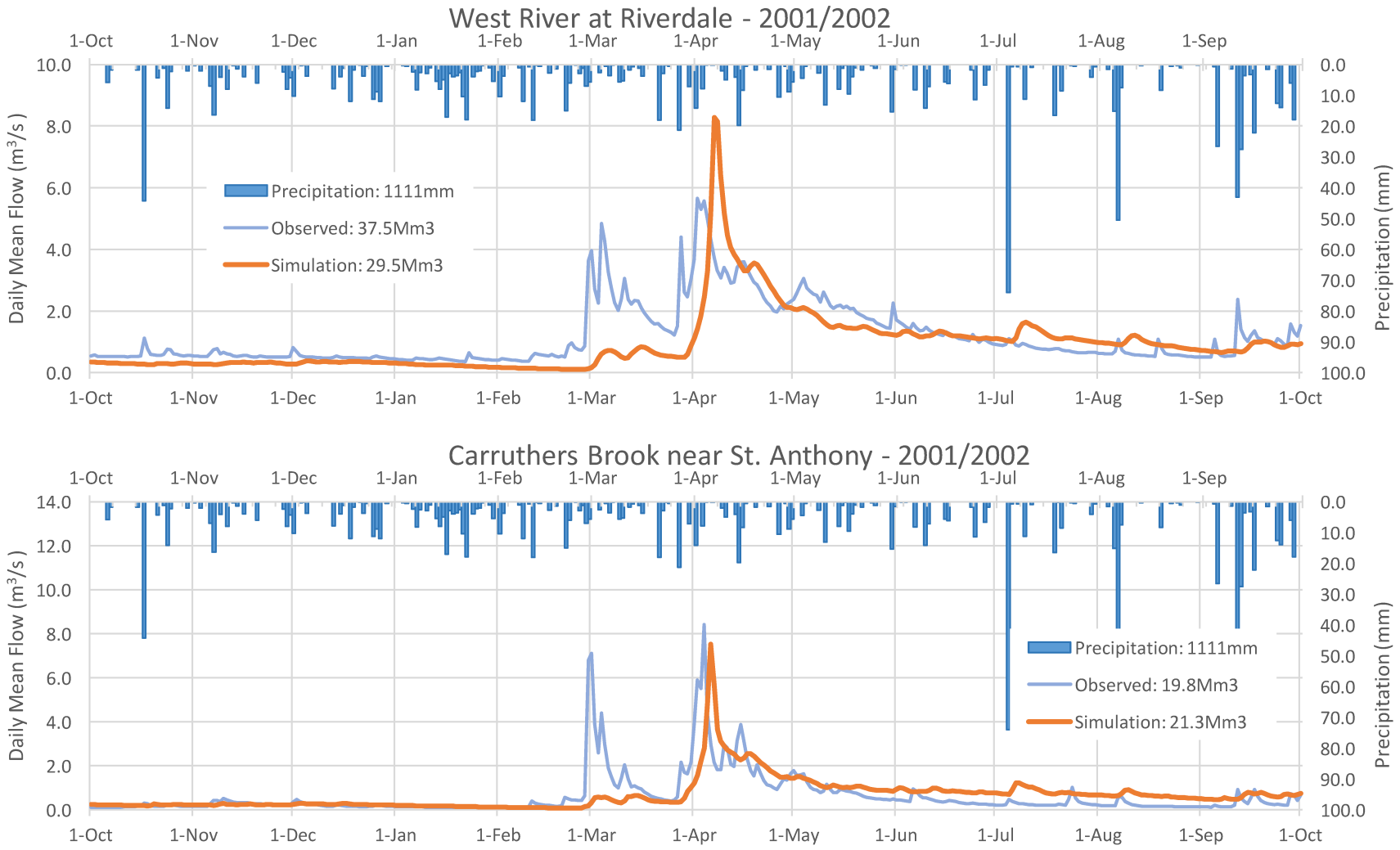

Figure 4.2 - Simulated vs observed flows for West River and Carruthers Brook for2000/01 (dry year). In both watersheds, observed data show the spring melt split into two events, while the simulated is one event timed with the latter.

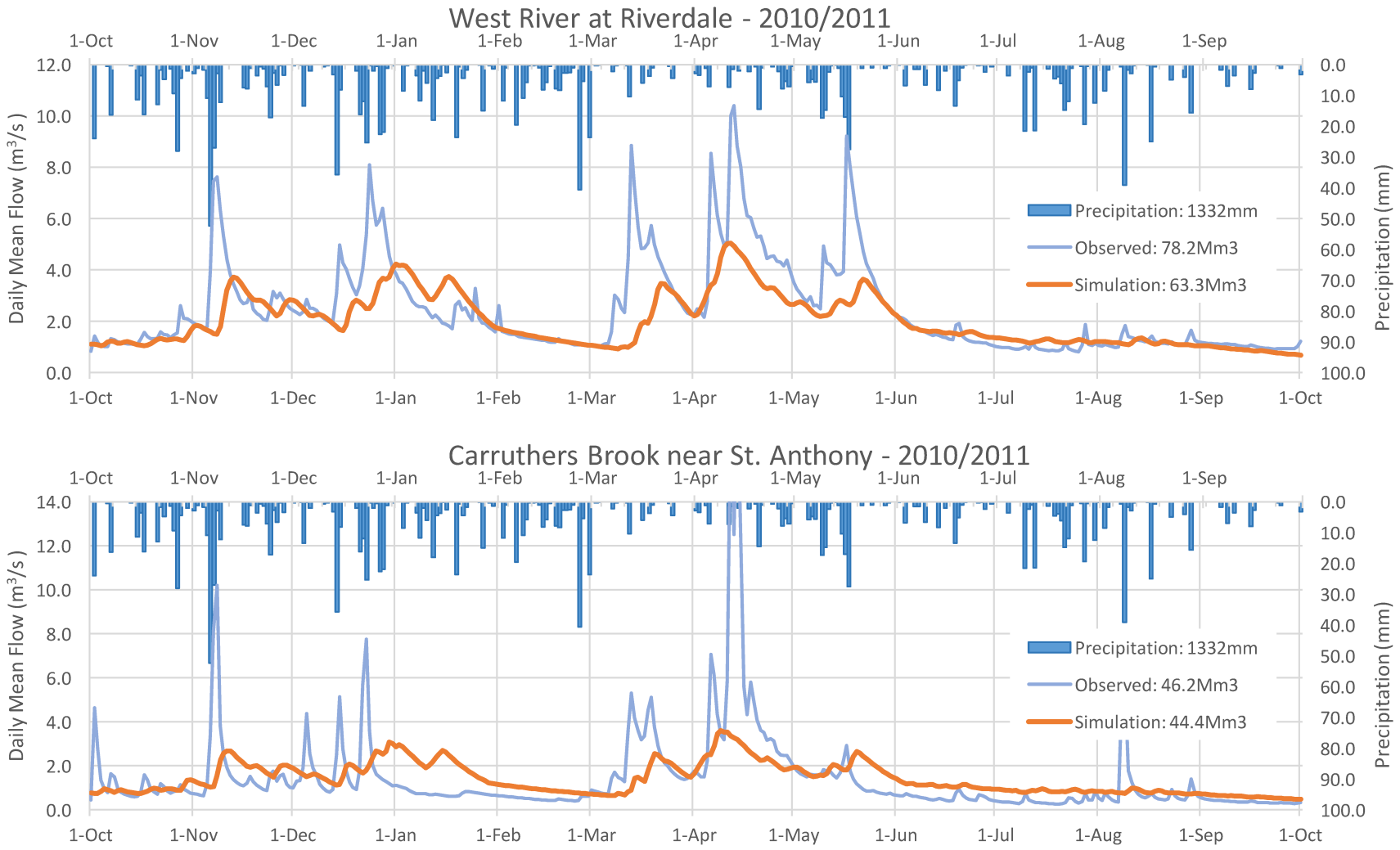

Figure 4.3 - Simulated vs observed flows for West River and Carruthers Brook for 2010/11 (wet year). In both watersheds, timing of winter flows events are reasonably simulated, but magnitudes are poor and consistently below observed.

Moriasi et al. (2007) recommended threshold values to determine satisfactory model performance for NSE and PBIAS of NSE > 0.5 and |PBIAS| < 0.25. However, these thresholds were for the statistics evaluated at a monthly time step, rather than the daily time step used in this model. PBIAS is not dependant on model time step, but NSE is and thus the threshold values should not be compared to results presented above. To determine if the simulation meets the "satisfactory" threshold, monthly NSE values for all validated runs were calculated by passing the mean monthly flow as input to the NSE statistic. These results are presented in Table 11.

Table 11 - Monthly NSE values for validated simulations. Runs marked in bold were selected for use in future modeling.

Max	*0.660*	*0.582*	*0.735*	*0.757*	*0.639*
Run #	**Dunk**	**Wilmot**	**West**	**Carruthers**	**Winter-L**
2228	**0.611**	**0.431**	**0.653**	**0.702**	-
1571	0.517	0.404	0.550	0.688	-
3488	0.503	0.381	0.571	0.590	-
2091	0.525	0.341	0.642	0.719	-
1139	0.556	0.416	0.601	0.684	-
1289	0.306	-0.014	0.493	0.741	-
2154	0.424	0.219	0.518	0.734	-
1376	0.519	0.401	0.602	0.532	-
2678	0.551	0.399	0.575	0.738	-
3162	0.313	-0.064	0.610	0.618	-
2457	-	-	-	-	0.522
3162	-	-	-	-	**0.610**

Based on these results, the Dunk, West, Carruthers and Lower Winter watersheds meet the monthly NSE threshold for satisfactory simulations, with Carruthers Brook exceeding the higher "Good" threshold of NSE > 0.65 and |PBIAS| < 0.15. Wilmot River falls slightly below the "satisfactory" threshold for NSE, and when combined with the significantly lower OBJ scores, the simulation for this watershed was not used in future modeling.

4.3 Future Climate Data Screening Assessment

Four GCMs were assessed to determine modelling skill specifically in the study area: GFDL, MRI-CGCM3, CNRM and MIROC5. Hindcast data from these four models were then compared to observation data at Charlottetown for the historical period 1980-

2005. Table 12 shows the calculated average daily error for precipitation and average temperature by month.

Table 12 – Average daily GCM errors for historical Charlottetown climate (1980-2005).

a) Precipitation (mm)

Month	GFDL	MRI-CGCM3	CNRM	MIROC5
Jan	-0.23	-0.02	0.19	0.21
Feb	0.07	0.09	0.00	-0.09
Mar	-0.06	-0.20	0.03	0.02
Apr	-0.22	-0.18	-0.14	-0.19
May	-0.07	0.21	-0.05	-0.29
Jun	-0.50	-0.70	-0.41	-0.30
Jul	0.16	0.04	-0.01	-0.10
Aug	-0.74	-0.26	-0.26	-0.18
Sep	-0.17	-0.46	-0.84	-0.85
Oct	-0.03	-0.26	-0.59	-0.11
Nov	-0.37	0.23	-0.12	0.07
Dec	-0.37	-0.44	-0.47	-0.74
Mean	*-0.21*	*-0.16*	*-0.22*	*-0.21*
Mean Error	0.25	0.26	0.26	0.26

b) Mean Temperature (˚C)

Month	GFDL	MRI-CGCM3	CNRM	MIROC5
Jan	1.07	0.39	0.30	2.03
Feb	2.57	0.42	0.41	2.53
Mar	2.03	-0.36	0.19	2.03
Apr	1.92	-0.36	-0.30	2.48
May	2.28	0.44	0.39	2.42
Jun	0.77	0.14	0.56	1.27
Jul	-0.72	0.16	0.19	-0.76
Aug	-1.65	0.09	0.40	-1.47
Sep	-1.25	0.23	0.39	-1.30
Oct	-2.23	0.50	0.59	-0.97
Nov	-1.62	0.40	-0.05	-1.25
Dec	*0.23*	*0.24*	*0.31*	*0.68*
Mean	1.55	0.36	0.37	1.64
Mean Error	1.07	0.39	0.30	2.03

The MRI-CGCM3 GCM was found to have the least error of the four and was therefore selected as the source for future climate data. To assess the full range of potential future climate, three scenarios were selected for analysis: RCP8.5, RCP4.5 and RCP2.6. These scenarios correspond approximately to minimal, moderate and major reductions in anthropogenic greenhouse gas emissions respectively.

4.4 Simulated Streamflow

The model calibration showed that the simulation of four of the five modeled watersheds performed best with the same parameter set. Given this, model results are expected to be very similar for all watersheds. The West River watershed performed best in calibration/validation and thus has been used to present results. The MRI-CGCM3 GCM with the RCP8.5 emission scenario has been used unless otherwise noted for these results, as it is the business as usual approach, and given current emission trends is likely to be best representative of the near-term future. Section 4.5 discusses and compares results from the other climate scenarios, while Section 4.6 examines variability associated with choice of GCM.

Given that the input future climate is only a simulation that has been statistically downscaled, individual years of model results should not be assessed to examine climate change. Natural climate variability is also significant at annual timescales. Therefore, flow results are presented using thirty year windows, moving decadaly. The thirty-year window allows for sufficient sample size to properly assess statistics of the distributions, while decadal increments allow sufficient overlap to show long-term change. Water balance components are presented via decadal averages to provide more resolution to change patterns and to better show variation that would otherwise be removed by thirty-year averaging.

For assessing seasonal variation, patterns in the mean monthly hydrograph were used to associate months with similar hydrological characteristics together into seasons. For this study, winter corresponds to the low-flow periods of December through March, when snow typically accumulates. Spring is defined as April and May, and represents

peak flows associated with snow melt. Summer is defined as June through August, when temperatures are highest and precipitation is low, while fall is comprised of the remaining months of September through November.

Median flows are useful for assessing the average flow conditions, however high and low flow periods are generally of more concern for planners and water managers. Four flow indicators have been selected to assess these changes: Q10, Q50, Q90 and Normalized Reference Base Flow (NRBF).

The Q10, Q50 and Q90 indicators are the flow that is exceeded 10%, 50% and 90% of the time respectively. Q90 is commonly used as a low-flow threshold, while Q10 is used as a peak (flood) threshold. The Normalized Reference Base Flow is an indicator that has been developed by the PEI government to assist in groundwater extraction permitting. The NRBF is the median flow from the summer low-flow period of 1-Aug to 30-Sep.

4.4.1 Comparison of Observed and Simulated Streamflow

Comparison of the observed flows with results from the historical simulation period show that while the model is generally able to produce satisfactory results, there are notable discrepancies. In terms of median monthly flows (Figure 4.4), summer flows are over-predicted by 19%, while winter, spring and fall flows are under-predicted (-23%, -12%, -27%). Likewise, cumulative seasonal/annual drainage (Figure 4.5) shows similar deviations, with a summer excess (+20%) offset by deficiency in the other three seasons (-15% to -22%) for a total annual under-prediction of -13%.

Compared to observed flows, the values of Q90, Q50 and NRBF for the simulation during the historical (1985-2014) period show little deviation, while the Q10 value is significantly reduced (-20%) (Figure 4.6). This corresponds well with the graphical assessment of the simulation, suggesting that low-flow periods are successfully modeled but high-flow events are reduced in magnitude and extended in duration to approximately balance volume.

Groundwater is an important source of base flow to streams. To quantify this for the study watersheds, the contribution from the HRU_{LZ} layer (groundwater) to stream flow

was calculated for the historical 1985-1994 period (Figure 4.7). These results show that groundwater provides 66% of the annual stream flow, while during the July through September low-flow period, groundwater provides 90% of the streamflow. These results agree with the work of Francis (1989) who found that groundwater provides approximately two thirds of annual stream flow and up to 100% during low flow periods in late summer and early fall.

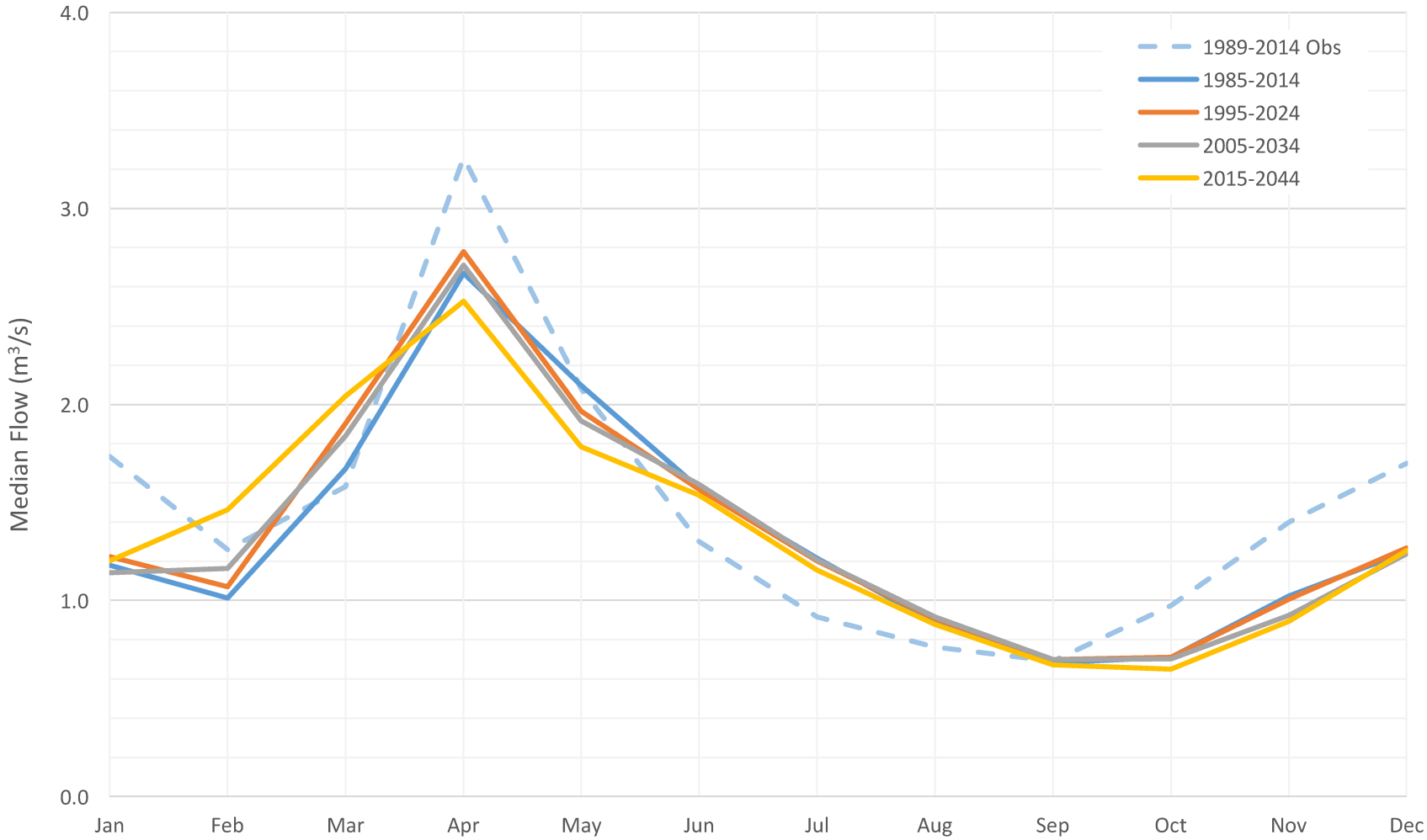

Figure 4.4 - Median monthly flow change for West River RCP8.5.

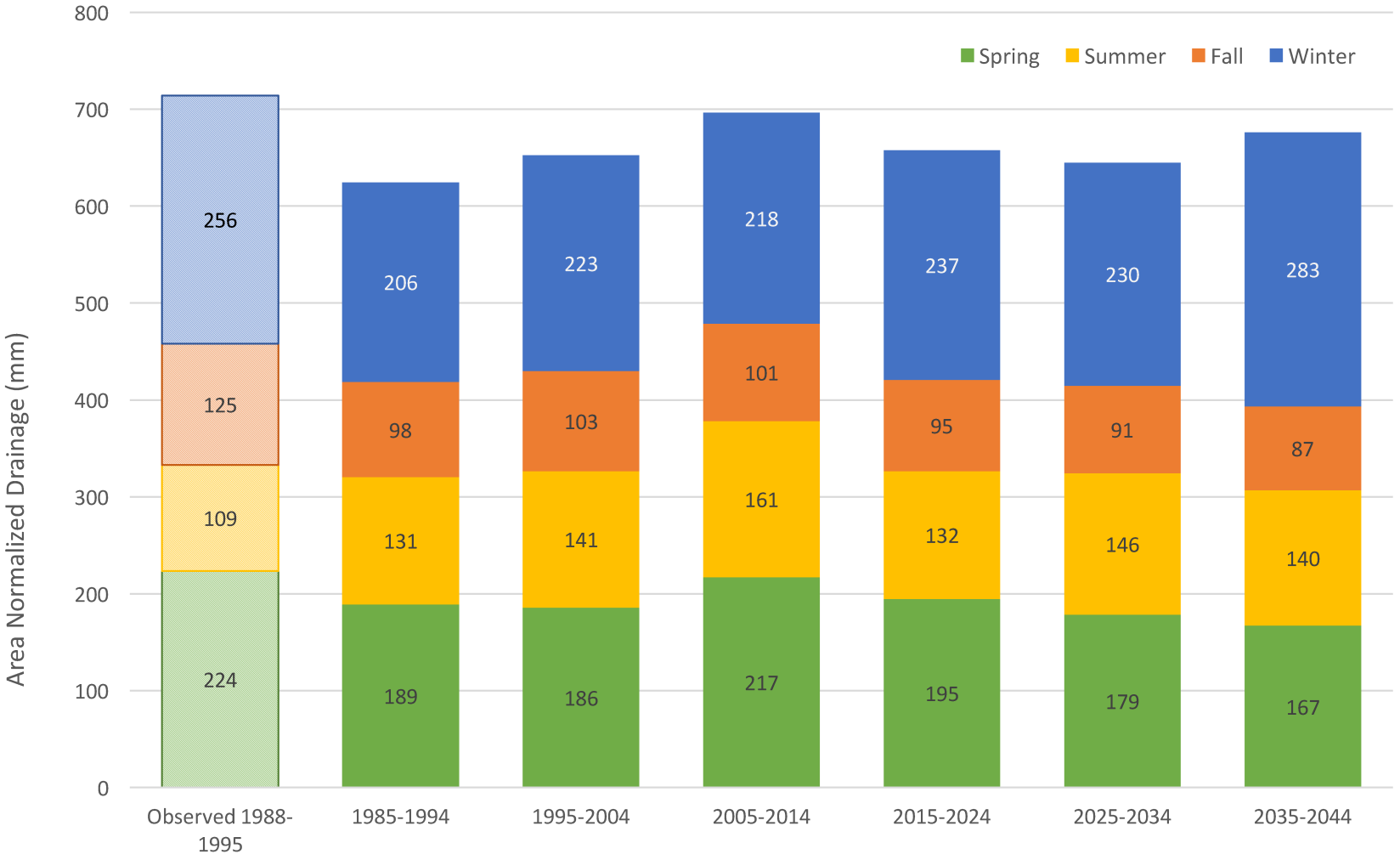

Figure 4.5 - Seasonal drainage change.

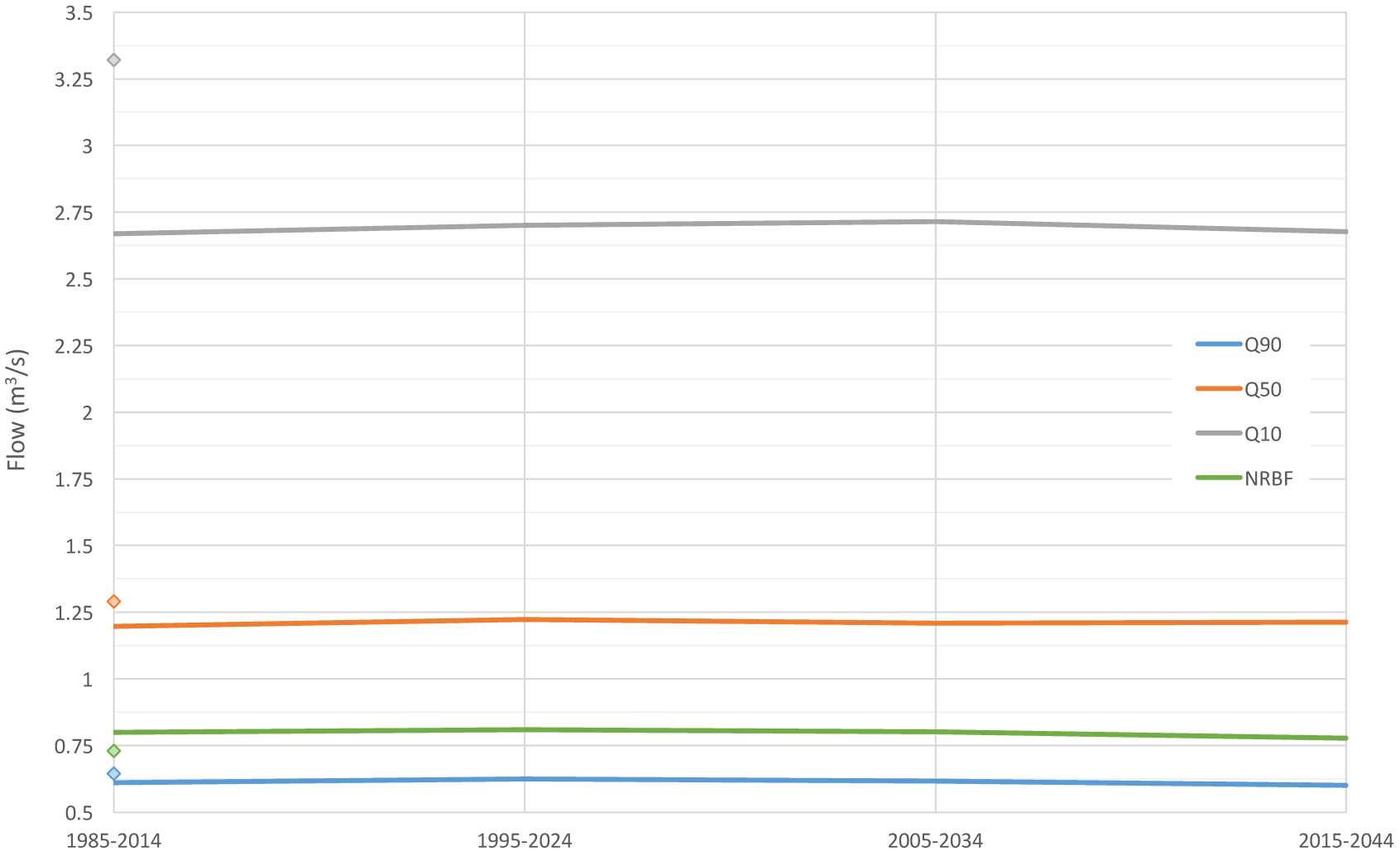

Figure 4.6 - Flow indicator change for West River RCP8.5. Indicator values from observed record are shown as points for reference.

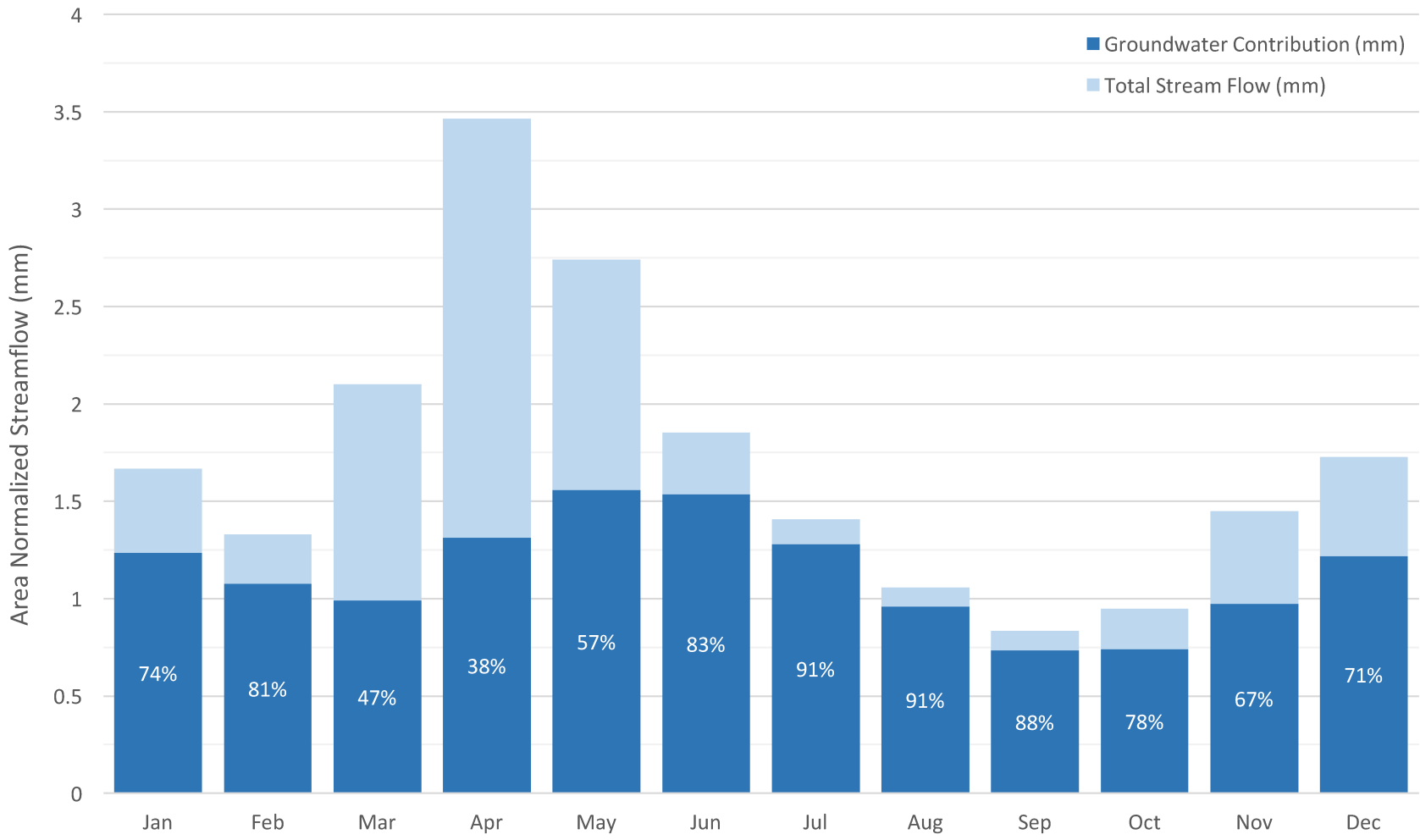

Figure 4.7 - Groundwater contribution to stream flow for West River RCP8.5 in the 1985-1994 baseline period.

4.4.2 Future Streamflow Change

To assess the change to future streamflow, median monthly flows were first examined and results show that there is little change expected in the base-case scenario (Figure 4.4). Summer median flows show little change, while winter flows increase by 17% and spring and fall flows decrease moderately (-10%, -8%). Switching to cumulative drainage, the mean annual drainage increases by 8% (Figure 4.5). Broken down seasonally, the simulation shows that winter drainage increases by about a third (37%), while summer drainage increases slightly (7%) and spring and fall drainage decrease moderately (-12%). These results are nearly identical to those of Roberts et al. (2012), while the seasonal changes are similar to those observed by Boyer et al. (2010) in Quebec and Rivard et al. (2014) in Nova Scotia.

Although there are notable changes to seasonal flow patterns as described above, annual peak-flow and low-flow values as represented by the four flow indicators change very little (<3%) between 2000s and 2030s (Figure 4.6).

To determine the source of these changes, the simulated water balance was examined (Figure 4.8). These results clearly show that precipitation and runoff increase from 1990 to 2010 by approximately 70 mm, and then return back to 1990 levels. On the other hand, ET increases throughout the period, with an extra 24 mm (6%) of ET by 2040. This result agrees with the work of Rivard et al. (2014) in Nova Scotia. As a consequence of the increased ET, net recharge to deep groundwater (recharge minus groundwater contribution to stream flow) drops by 60%, from 27 mm to 11 mm. Given that PEI is highly dependent on groundwater for drinking water and that groundwater extraction was not included in this model, this major reduction to aquifer recharge is especially concerning.

In addition to its impact on the annual water balance, evapotranspiration is important for agriculture as increased ET can deplete soil moisture during the growing season and limit crop growth. To assess this, the average monthly soil moisture deficiency (difference between potential and actual evapotranspiration) was calculated for each decade of simulation (Figure 4.9). The results show that peak soil moisture deficiency in

August is not expected to change dramatically, however July and September both show large increases (6 mm, 4 mm). This suggests that the water stress season will likely expand both earlier and later.

Another effect of the changing climate is shown in winter snowpack volumes (Figure 4.10). Between 1985 and 2034, decadal snow water equivalent (SWE) averages vary significantly (by 32%) but do not show any consistent trend, suggesting that random annual climate variation is dominant. However, the final 2035-2044 decade shows a major (65%) drop in maximum annual SWE, and is consistent across all winter months. This agrees with the work of Rivard et al. (2014) who reported the amount of precipitation falling as snow dropped by over half by the 2050s in their Nova Scotia study.

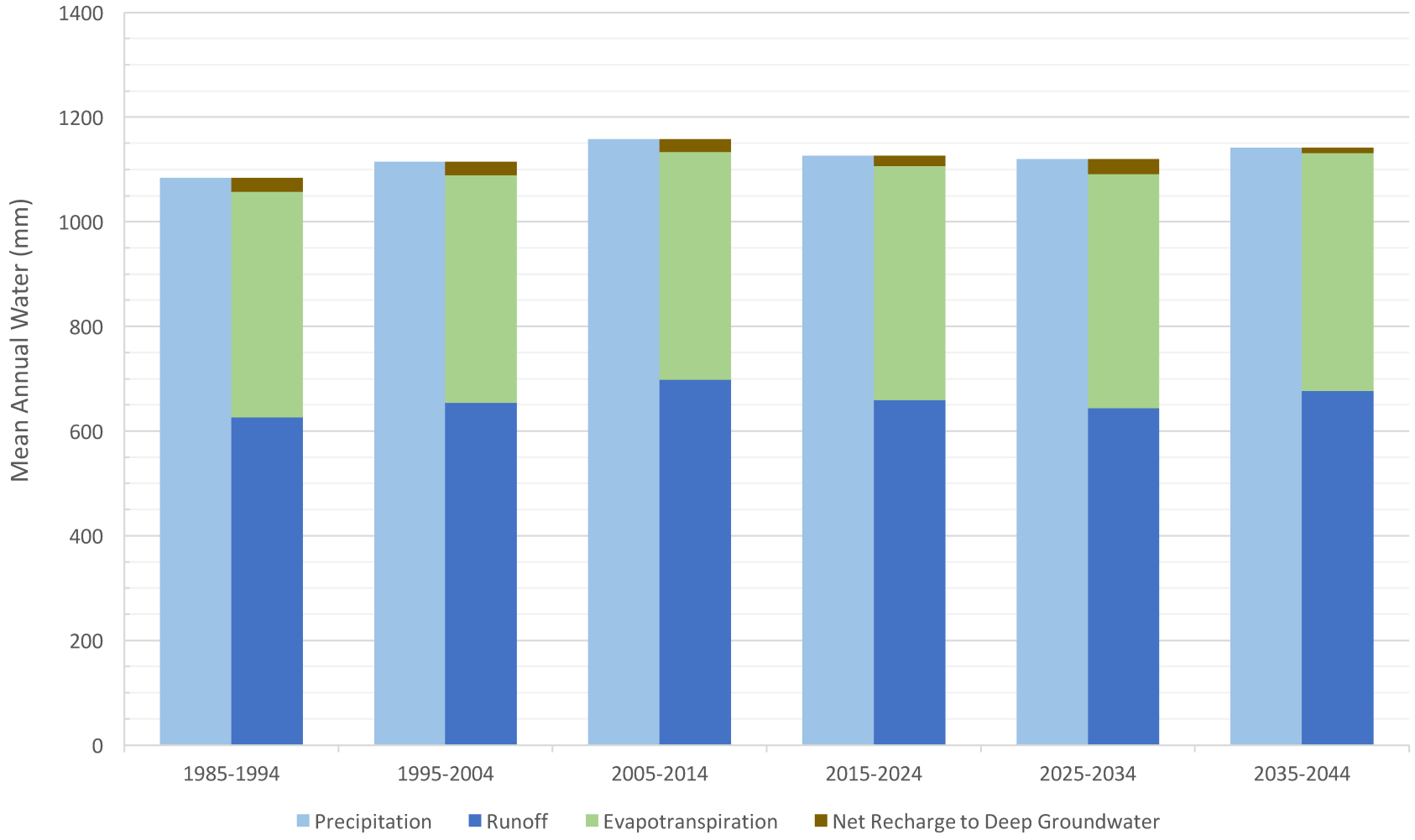

Figure 4.8 - Water balance change.

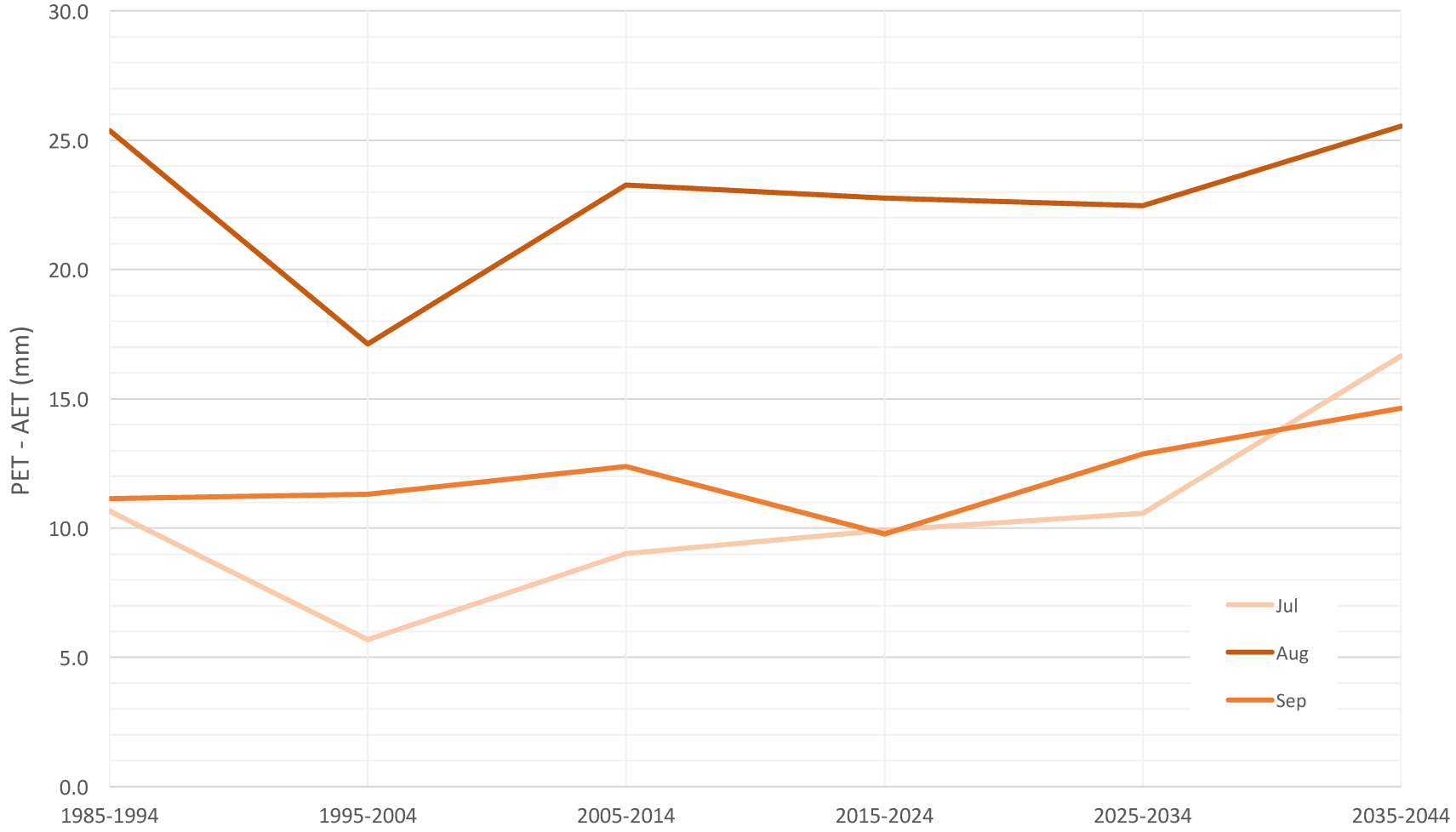

Figure 4.9 - Soil moisture deficiency during summer months.

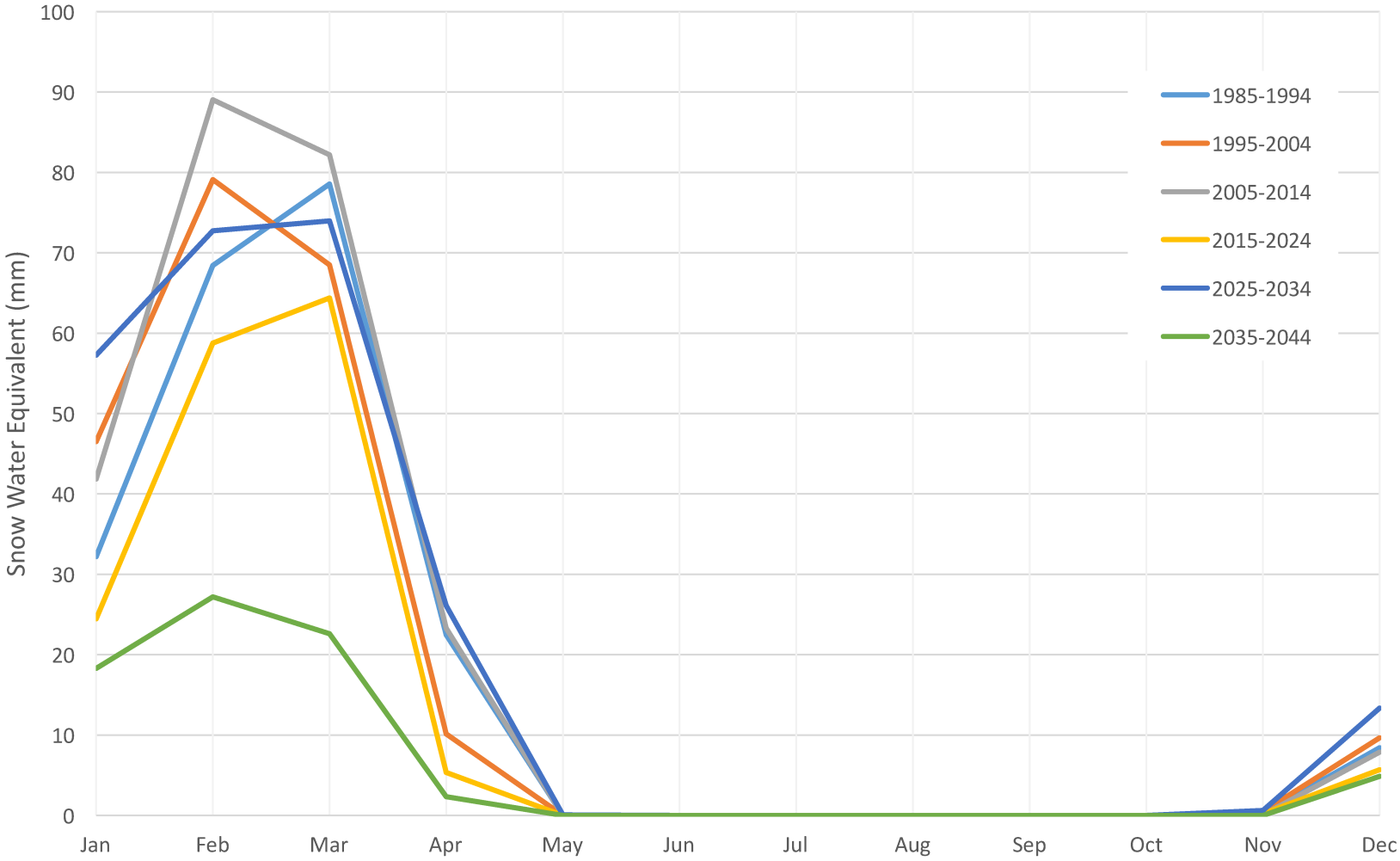

Figure 4.10 – Monthly maximum snowpack change over time..

4.5 Emissions Scenario Analysis

To assess uncertainty in the hydrological system due to emission scenario, the annual precipitation was first compared seasonally across periods and scenarios (Figure 4.11). At the annual timescale, this shows that by the end of the simulation, annual precipitation increases across all scenarios, with RCP2.6 increasing the most (15%) while RCP4.5 and RCP8.5 showed smaller increases (10%, 5%). Seasonally, winter precipitation shows the greatest increase over the baseline period in all three scenarios (18% to 26%), while fall precipitation shows the smallest seasonal increase (+4% in RCP2.6 & RCP 4.5) or a decrease (-16% in RCP8.5). Spring and summer precipitation are generally higher across scenarios (+10% mean, -4% to +19%). Overall, these results show that increased emissions are expected to lead to reduced annual precipitation, although the seasonality is not affected greatly as precipitation increases most across all scenarios in the winter and least in the fall.

Beyond the precipitation changes, the annual water balance data for the three scenarios show little variation (Figure 4.12). Evapotranspiration increases approximately 5% in each scenario matching results of Rivard et al. (2014), and the precipitation increases are accommodated by increases to runoff (8% to 23%). Net recharge to deep groundwater drops significantly in all three scenarios, though less in the wetter RCP2.6 and RCP4.5 scenarios (-29%, -19%) compared to the RCP8.5 scenario (-60%).

The major decrease in winter snowpack found in the base-case RCP8.5 scenario is seen across all emission scenarios (Figure 4.13). As expected, the warmer RCP8.5 scenario results in the greatest peak snowpack reduction (-65%), but the RCP2.6 and RCP4.5 scenarios also show large decreases (-57%, -40%).

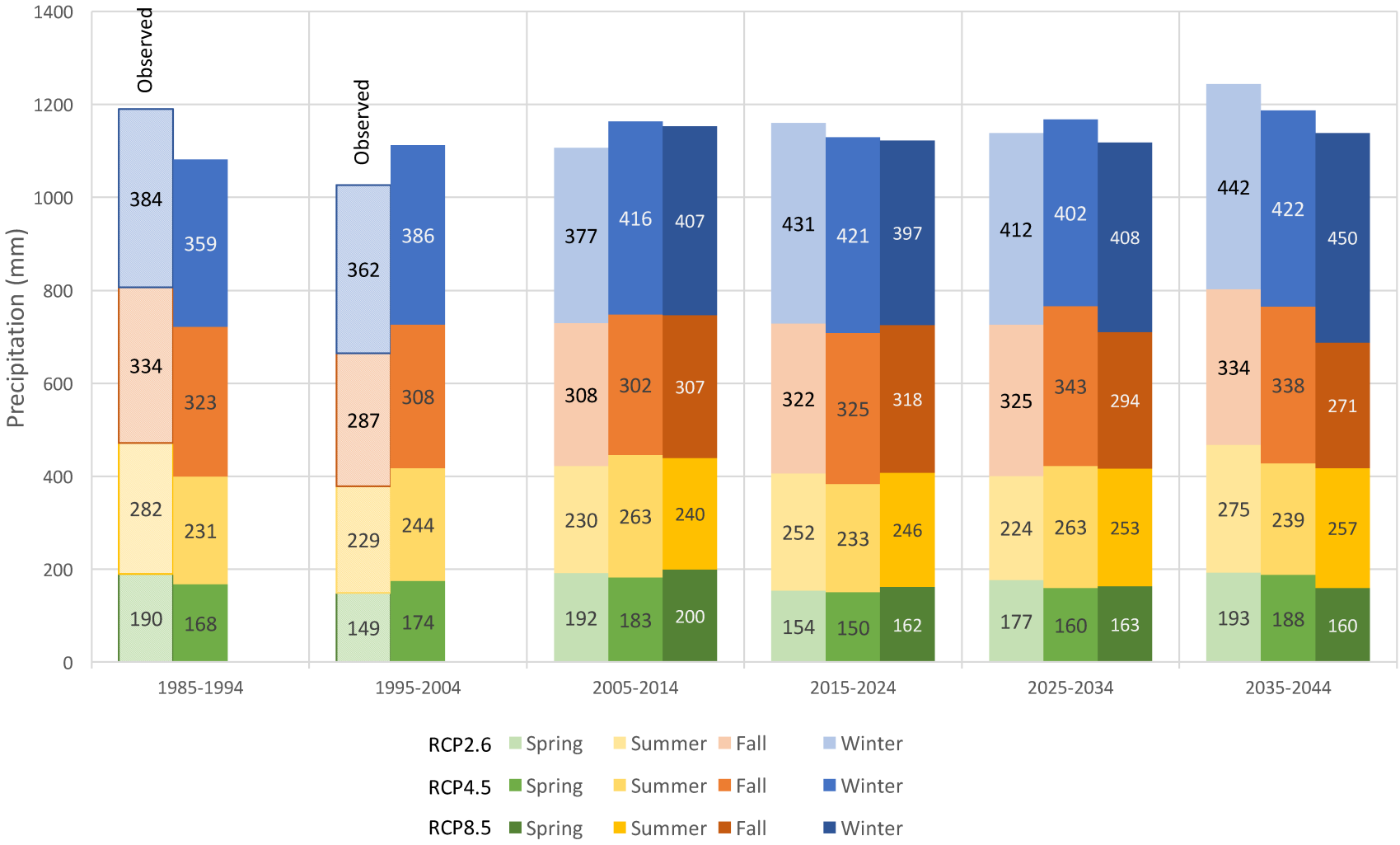

Figure 4.11 - Seasonal precipitation change by emission scenario.

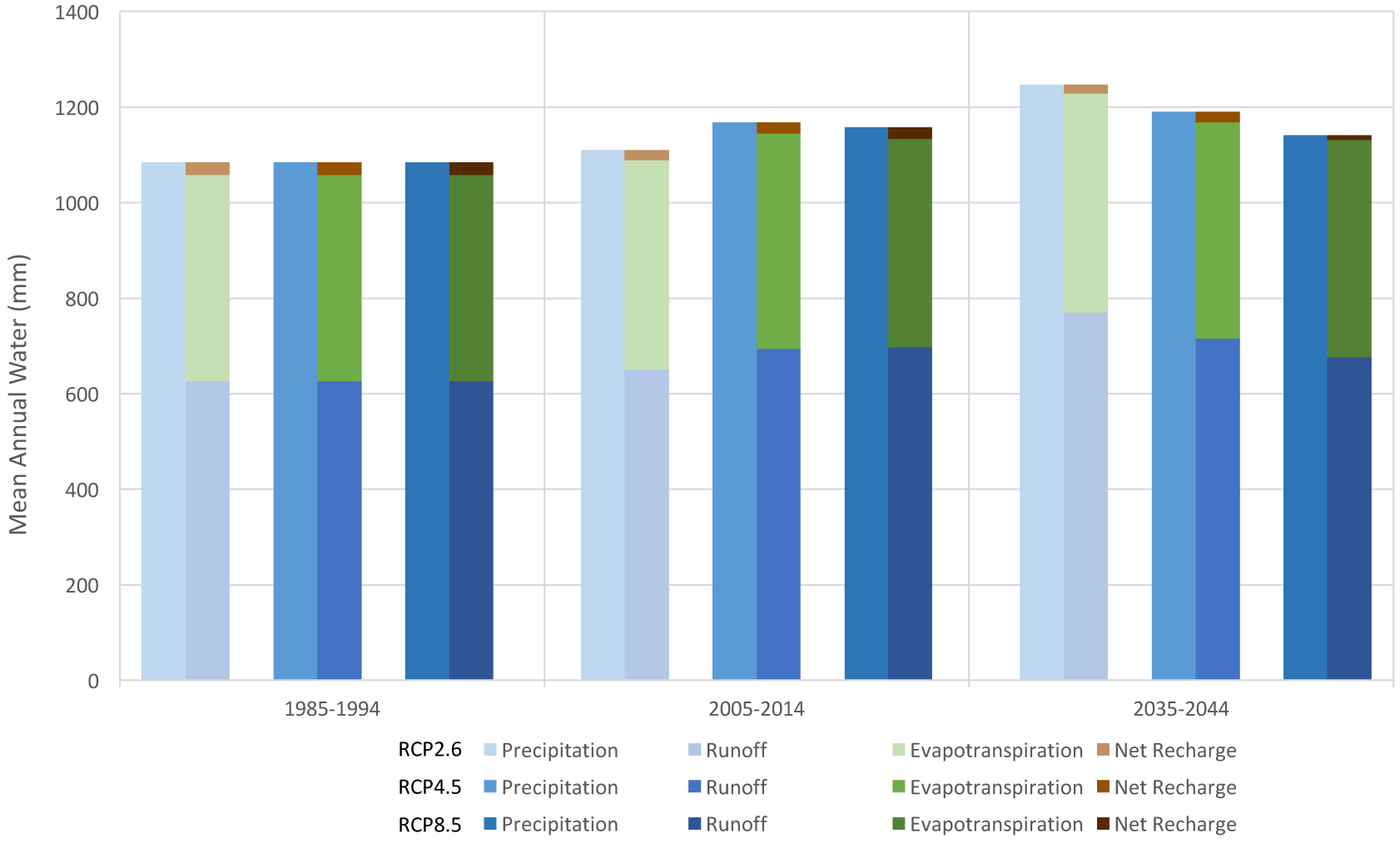

Figure 4.12 - Annual water balance change by emission scenario.

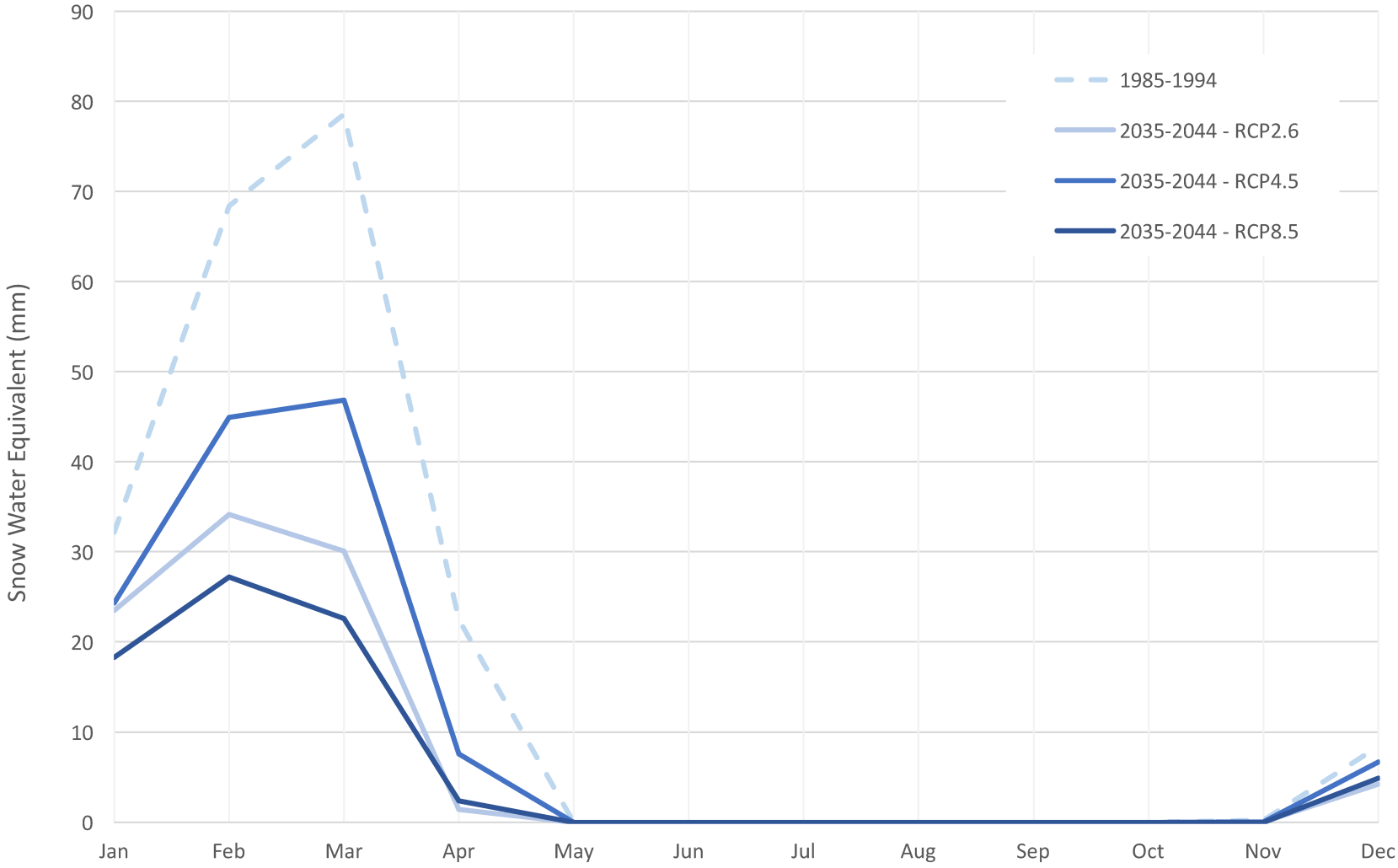

Figure 4.13 - Snowpack change by emission scenario.

To assess the impact of emission scenario on stream flows, median monthly stream flows were calculated for each scenario in both the baseline (1985-2014) and future (2015-2044) periods (Figure 4.14). Median monthly flows are largely consistent across emission scenario, with all three scenarios showing nearly no change in summer and fall, while there is a consistent increase in winter flows and a consistent drop in spring melt flows. The RCP2.6 scenario shows higher monthly median flows however this is expected given the increased precipitation in this scenario.

The seasonal drainage data (Figure 4.15) mirror the median flow values well, with RCP8.5 showing lower drainage in all seasons compared to both other scenarios. Winter drainage increases in all three scenarios (28% to 48%)

The hydrological indicators show similar trends across the three emissions scenarios (Figure 4.16). NRBF shows very little change across time and scenario, while Q90, Q50 and Q10 all show little change but the values in RCP2.6 are consistently higher than other scenarios, likely due to the increased precipitation.

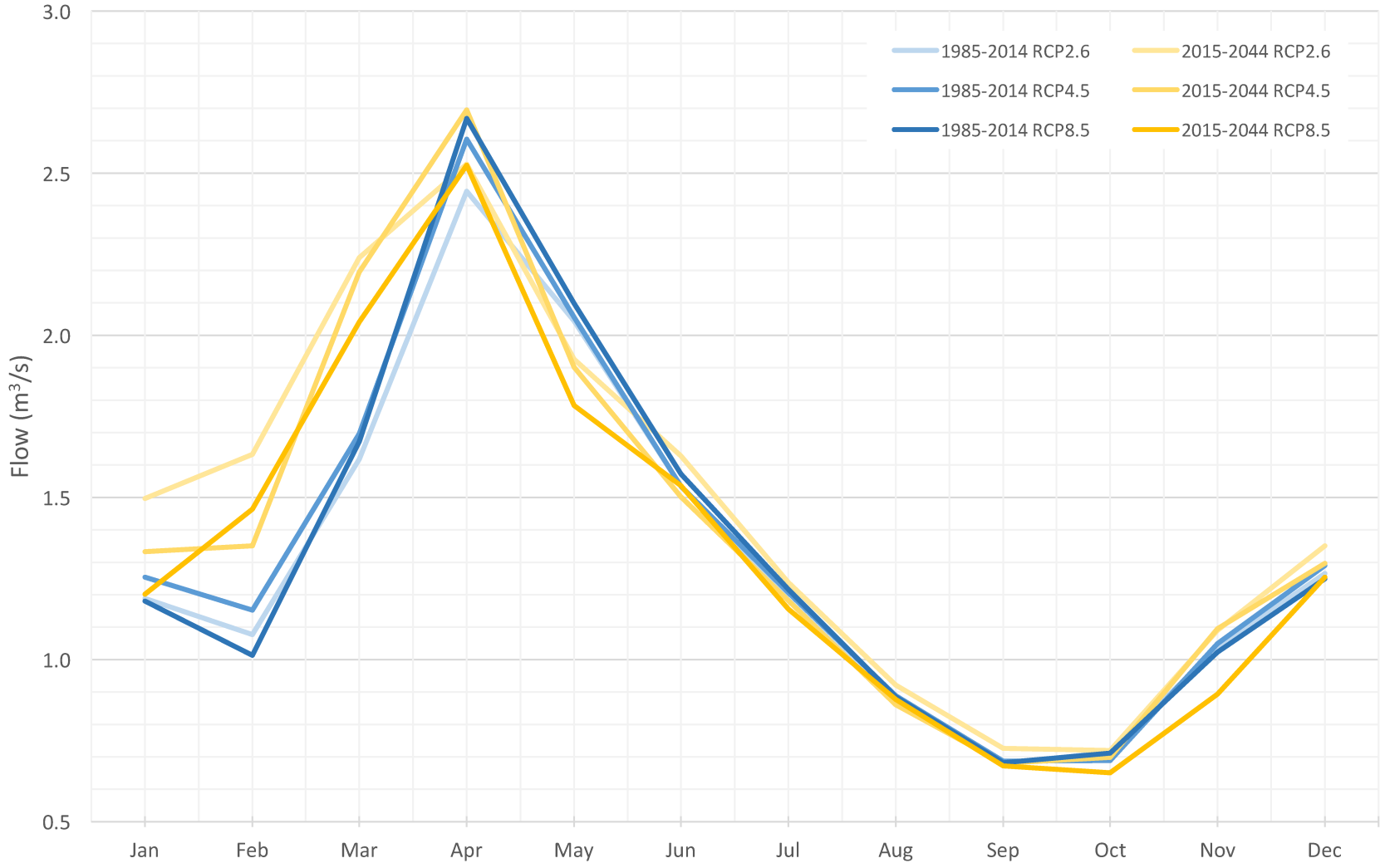

Figure 4.14 - Median monthly flow change by emission scenario.

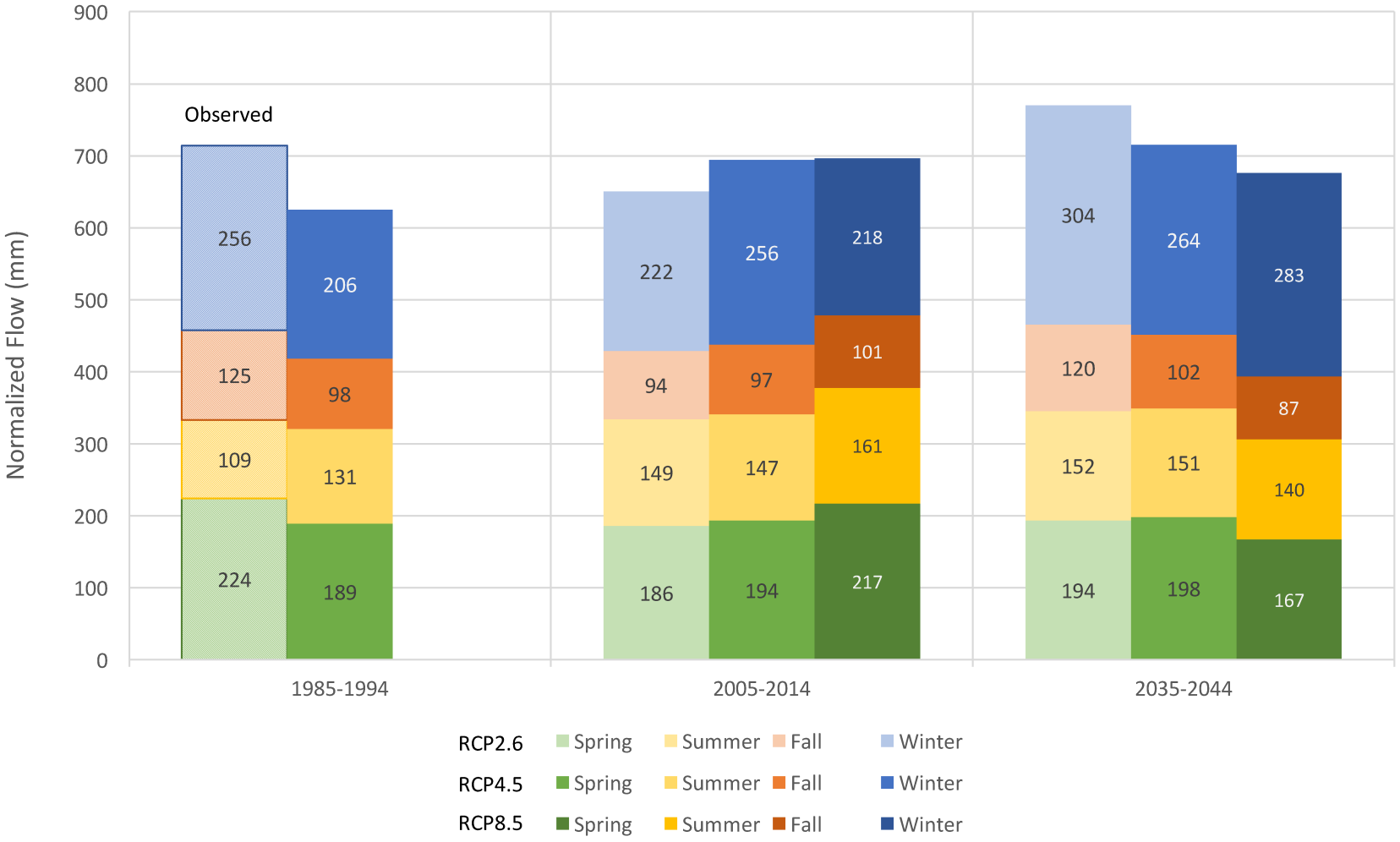

Figure 4.15 - Seasonal drainage change by emission scenario.

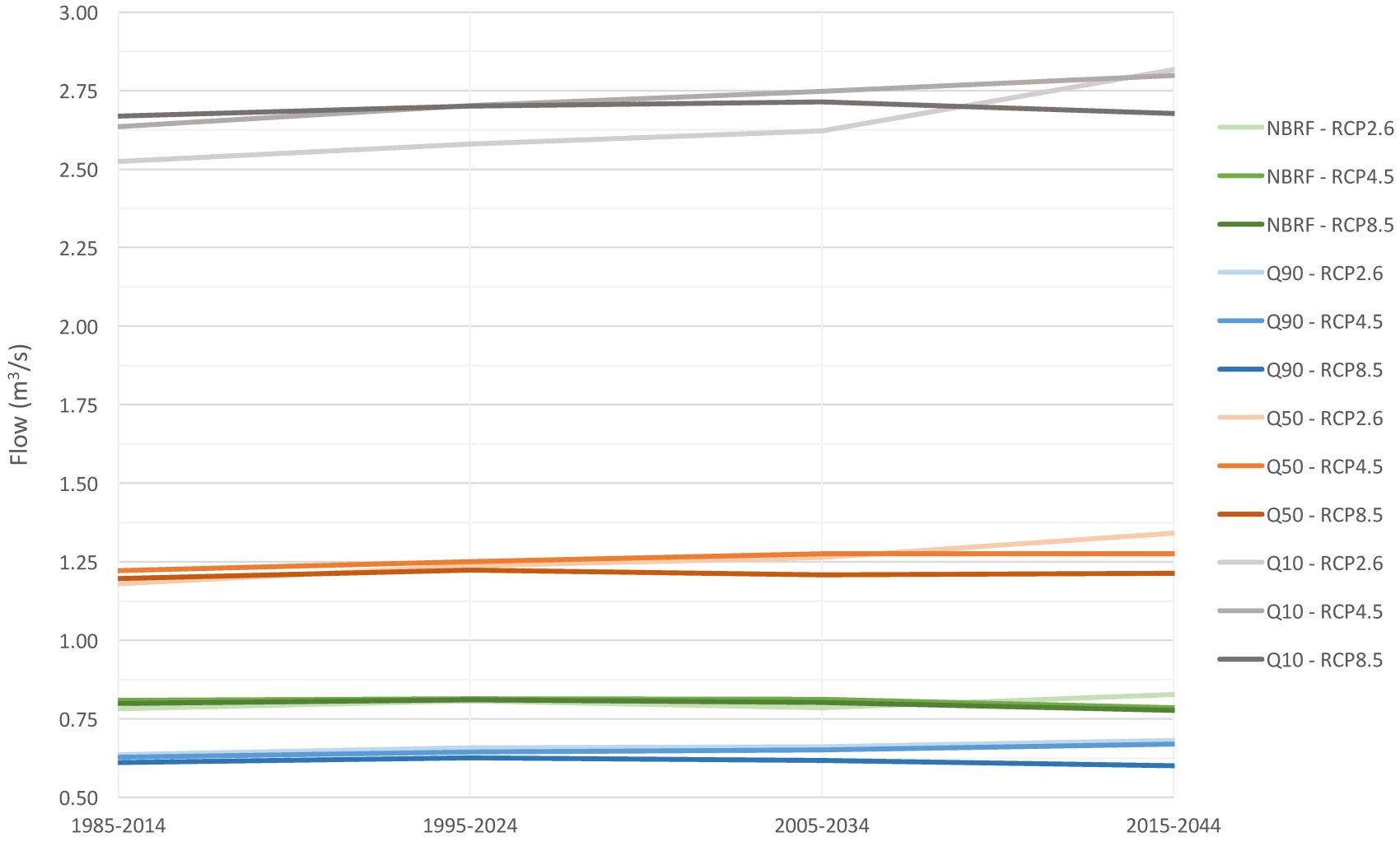

Figure 4.16 - Streamflow indicator change by emission scenario.

4.6 GCM Sensitivity Analysis

To assess the uncertainty due to GCM selection associated with model results, BCCAQ statistically downscaled future climate data from three other GCMs (CNRM, GFDL, MIROC5) was used as input to the hydrological model for the RCP8.5 emissions scenario. Figure 4.17 shows the variation between GCMs for the annual water balance for the 2035-2044 period. While precipitation estimates vary by 150 mm (13%), the runoff coefficient (runoff as a proportion of precipitation) shows little variation across GCMs (Table 13). This indicates that the are no major changes in hydrological processes or limits at the annual timescale across the various scenarios, as increased precipitation results in a proportional increase in flow.

Table 13 - Runoff coefficient change by period for each GCM.

Runoff Coefficient	CGCM	CNRM	GFDL	MIROC5
1985-1994	0.58	0.57	0.58	0.57
1995-2004	0.59	0.57	0.57	0.57
2005-2014	0.60	0.57	0.57	0.60
2015-2024	0.59	0.59	0.60	0.58
2025-2034	0.58	0.58	0.57	0.56
2035-2044	0.59	0.58	0.59	0.57

To confirm the significant reduction in winter snowpack identified in the initial results, snowpack volumes were analysed for all four GCMs (Figure 4.18). While the timing and volume of maximum snowpack varies between GCMs, all four show major reductions in peak snowpack volumes, ranging between -40% and -70%.

With respect to median flows, there is again little variation between GCMs (Figure 4.19). The main differences are related to the spring melt; both the GFDL and MIROC5 GCMs show peak spring melt flows occurring earlier in the year (March versus April), and the GFDL model shows an 11% increase in median flow at the peak of the spring melt compared to CGCM.

The four GCMs also do not show major variation in the streamflow indictors (Figure 4.20). The MRI-CGCM3 and MIROC5 models showed very little change to any of the

indicators between the historic and future periods, while Q90 with the CNRM model and Q10 with the GFDL model increased slightly (13%, 12%).

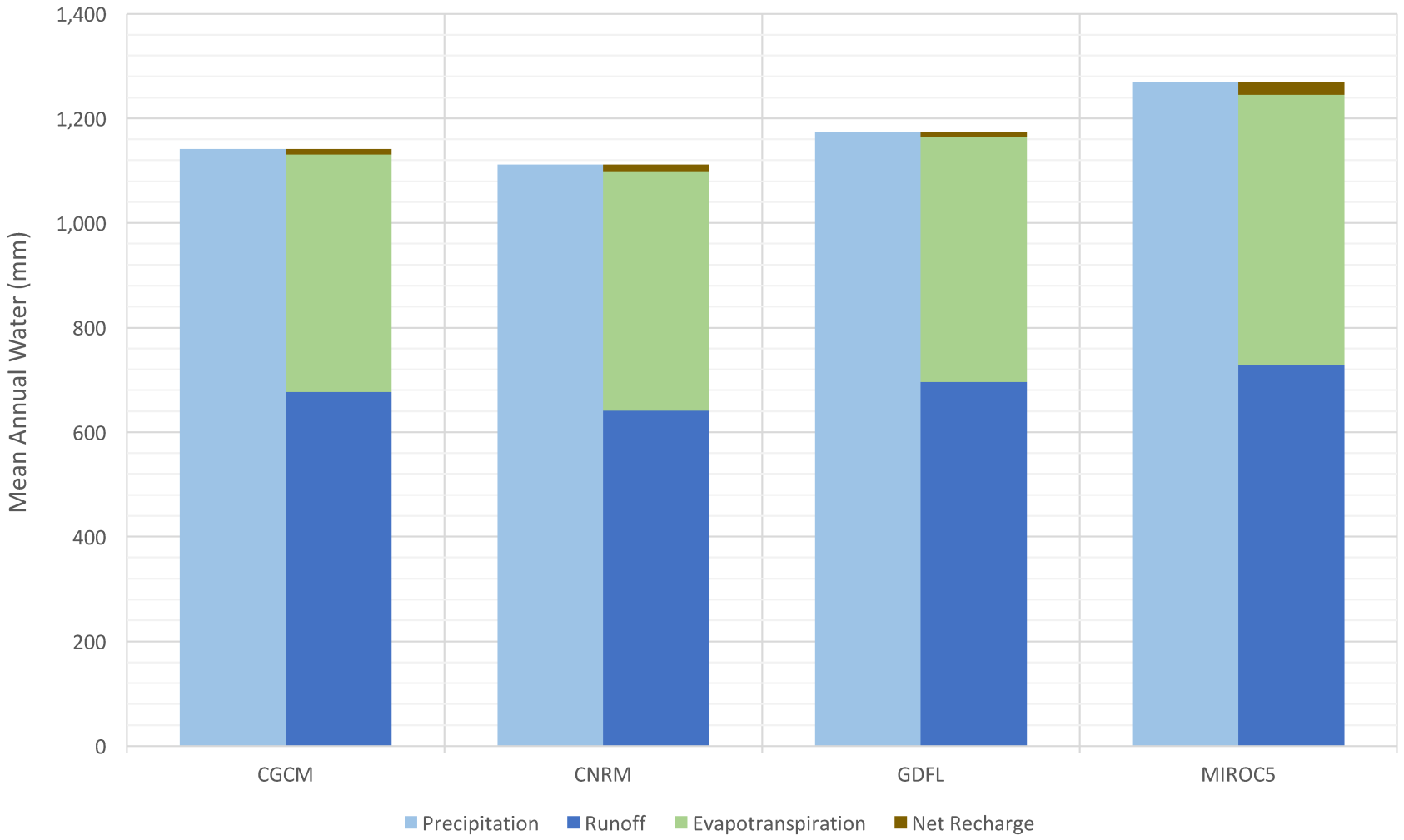

Figure 4.17 - Water balance variation across GCMs for the 2035-2044 period.

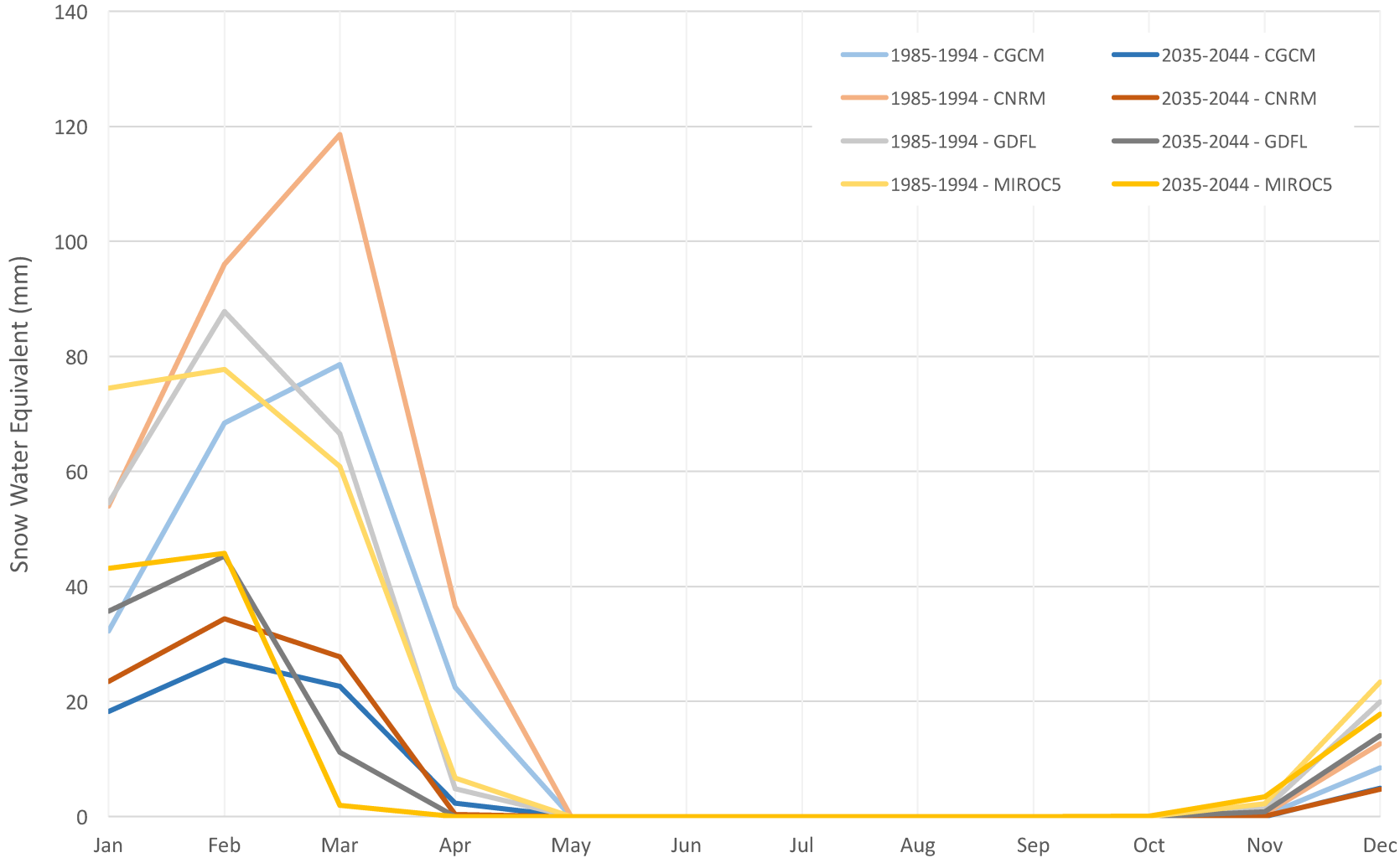

Figure 4.18 - Snowpack change variation across GCMs.

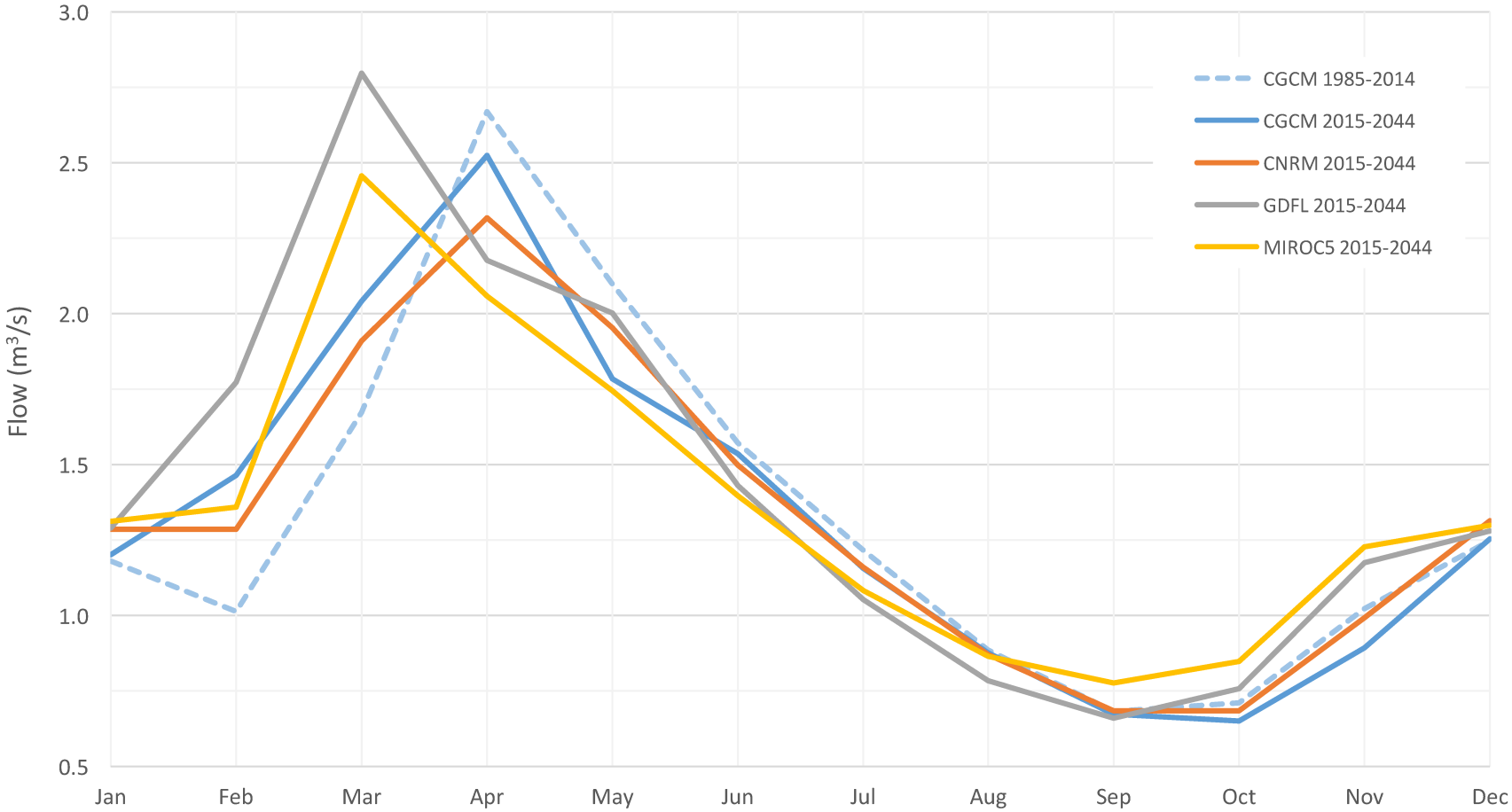

Figure 4.19 - Median monthly flows for the period 2015-2044 across four GCMs.

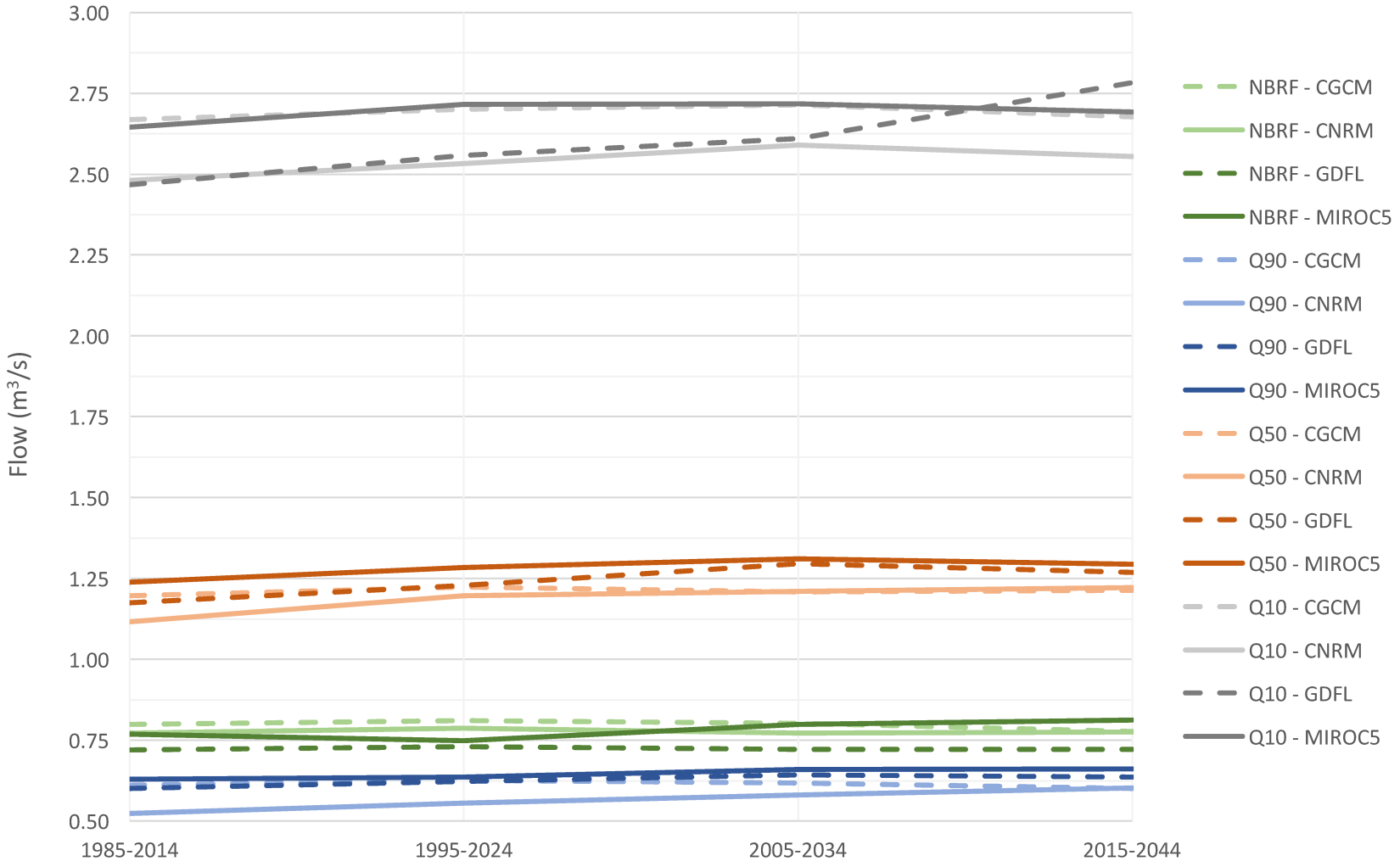

Figure 4.20 - Streamflow indicator change by GCM.

4.7 Drought Assessment

The drought assessment was carried out for the West River watershed. Three datasets were examined in the 25-year historical period (1990-2014): calibration representing the calibrated hydrological model using observed Charlottetown climate data, observation representing the observed flow data from the stream gauge, and simulation representing the calibrated hydrological model using the statistically downscaled gridded climate data from the MRI-CGCM3 GCM. Six datasets were assessed from the 30-year future period (2015-2044), one for each of the three emission scenarios (RCP8.5, RCP4.5 & RCP2.6) using the MRI-CGCM3 GCM, and one for each of the three GCMs used in the climate sensitivity analysis (CNRM, GFDL & MIROC5) with each using the RCP8.5 emission scenario.

When fitting the observed annual minimum series data from the observed record, the flow from 2013 was well below the other years for both the 7Q and 60Q indicators. This year was deemed an outlier and excluded from the distribution fitting. Overall, the fit of the distributions to the samples was satisfactory, with Kolmogorov-Smirnov values ranging between 0.08 to 0.17.

The results of the drought assessment are presented in Table 14. In general, the 7Q10 and 60Q50 indicators both follow similar patterns across all of the assessed datasets. The values for the historical simulation dataset are 15% and 25% lower than the observed dataset for the 7Q10 and 60Q50 respectively, suggesting that the simulations generate more extreme low flows, but the deviation from observed is not very large and thus the simulation appears to be appropriate.

Table 14 - Drought indicator values for West River.

Period	7Q10 (m^3/s)	K-S Value	60Q50 (m^3/s)	K-S Value
Calibration	0.37	0.130	0.34	0.094
Observation	0.50	0.123	0.58	0.103
Simulation 1990-2014	0.43	0.129	0.44	0.145
Simulation 1985-2014	0.42	0.122	0.43	0.148
Simulation 2015-2044 RCP2.6	0.40	0.091	0.38	0.087
Simulation 2015-2044 RCP4.5	0.43	0.087	0.42	0.084
Simulation 2015-2044 RCP8.5	0.41	0.090	0.42	0.080
Simulation 2015-2044 CNRM	0.41	0.113	0.42	0.114
Simulation 2015-2044 GFDL	0.40	0.105	0.34	0.118
Simulation 2015-2044 MIROC5	0.36	0.136	0.42	0.146

For the 7Q10 indicator (Figure 4.21 & Figure 4.22), the choice of emission scenario does not have a large effect on the expected low-flow, with all three scenarios showing change of less than 5%. Two of the other GCMs also give similar results for the 7Q10 indicator, however the MIROC5 GCM data gives a 7Q10 flow that is 9% below historical. This may be related to differences in the annual minimum series from the MIROC5 GCM which shows a distinct slope break at 3.3 years return period rather than all other simulations which were generally below 2 years.

The 60Q50 indicator shows more variability between GCMs and emission scenarios (Figure 4.23 & Figure 4.24). Overall, the expected low-flow drops in all scenarios compared to the historical simulation, however the change is less than 7% for MRI-CGCM in the two higher emission scenarios and the CNRM RCP8.5 scenario. The MRI-CGCM RCP2.6 scenario shows a 13% drop in expected low-flow, while the GFDL and MIROC5 GCMs under the high emission scenario drop sharply by 22% and 28% respectively. As with the 7Q10 indicator, the annual minimum series from the MIROC5 GCM was markedly different than other scenarios.

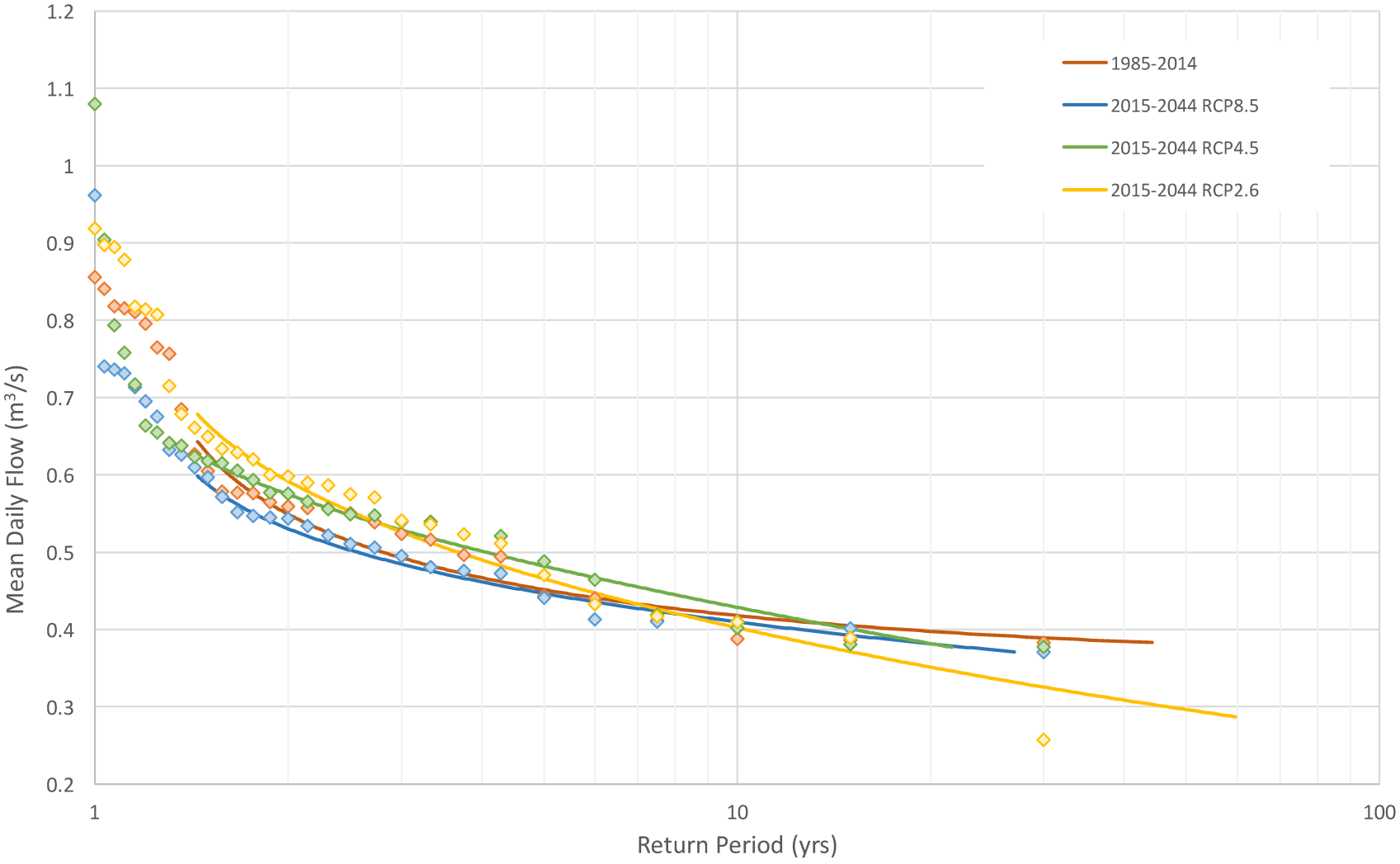

Figure 4.21 – Severity-duration-frequency curves for the annual 7-day summer/fall drought using three emissions scenarios.

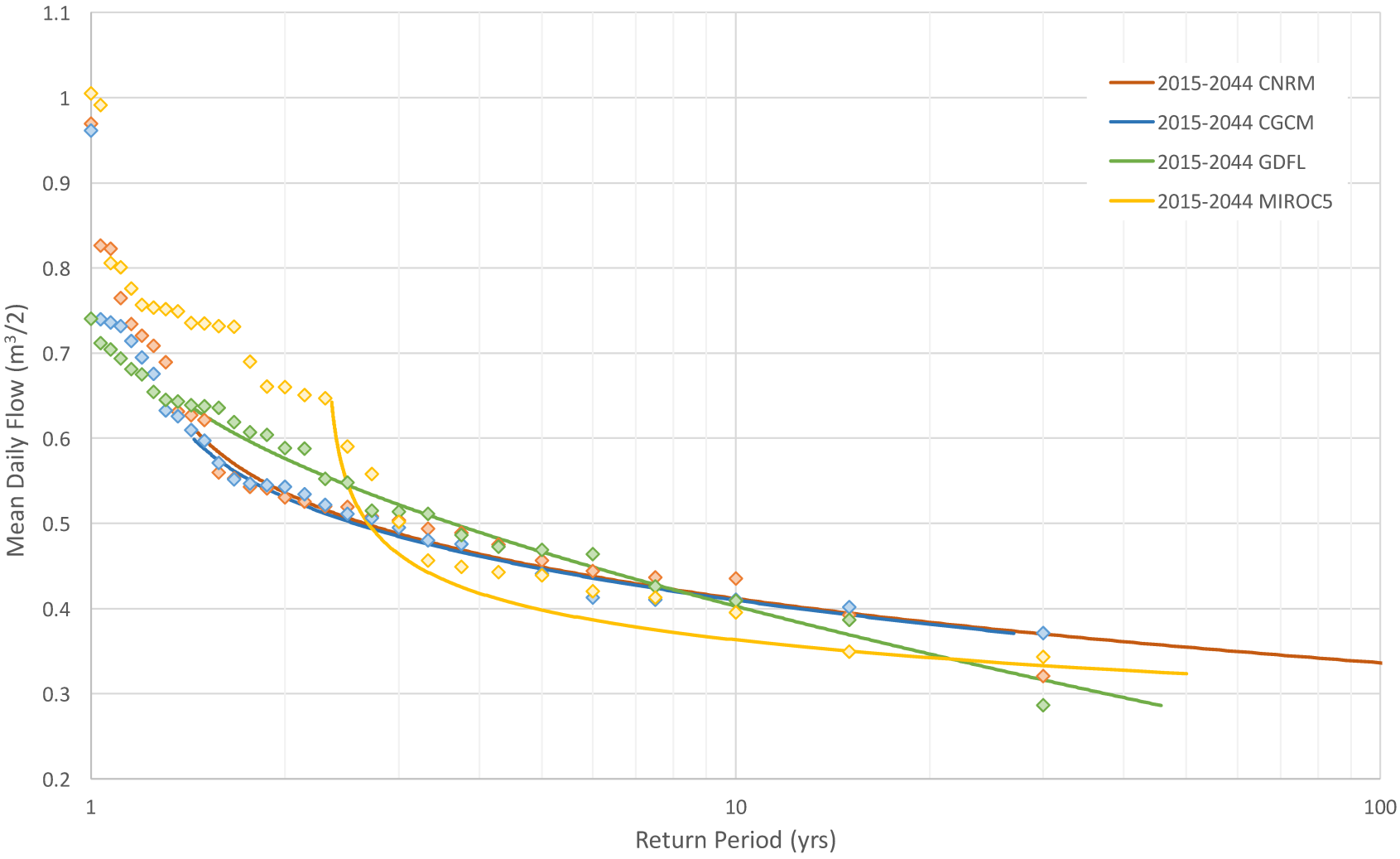

Figure 4.22 - Severity-duration-frequency curves for the annual 7-day summer/fall drought using four different GCMs.

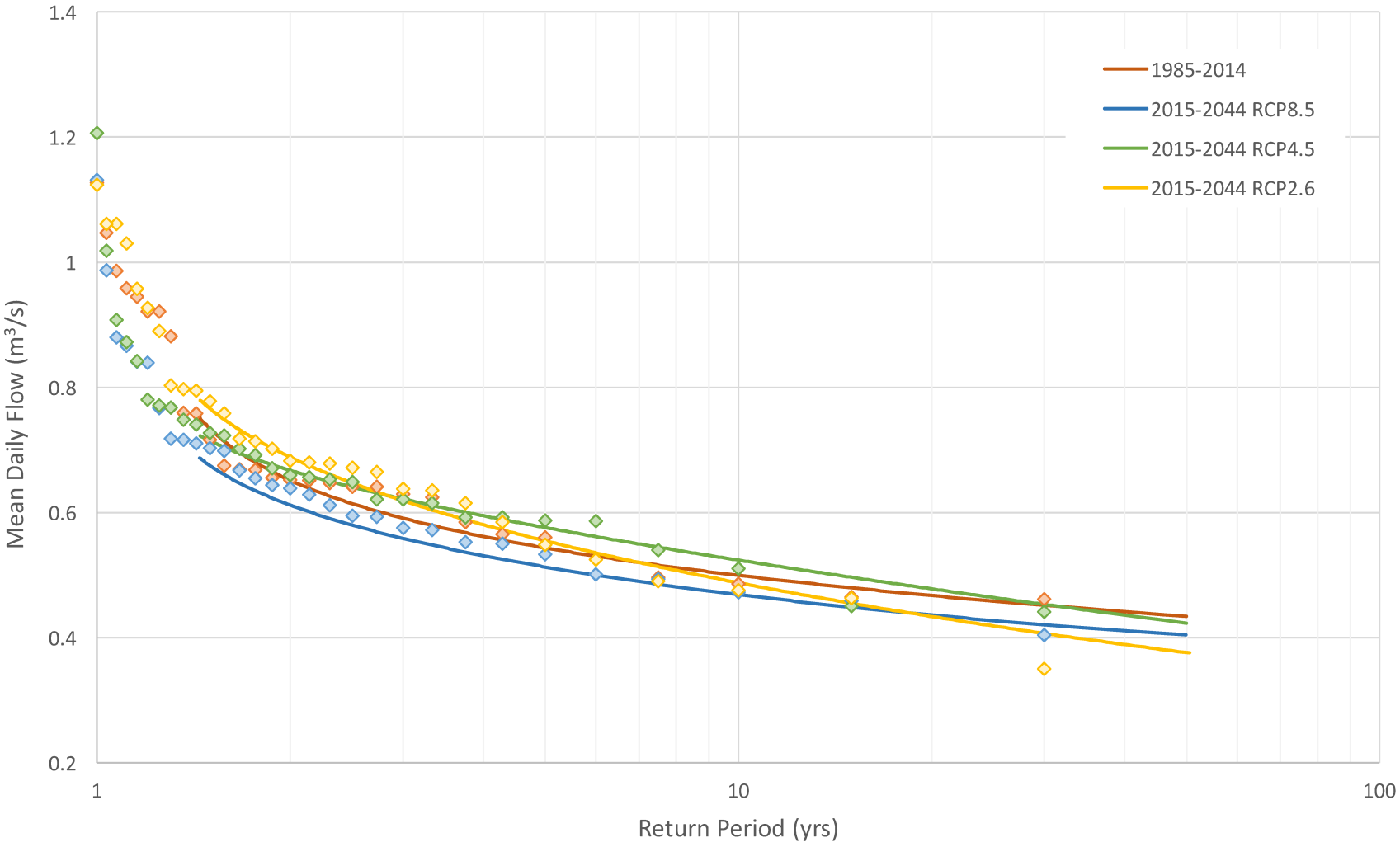

Figure 4.23 - Severity-duration-frequency curves for the annual 60-day summer/fall drought using three emission scenarios.

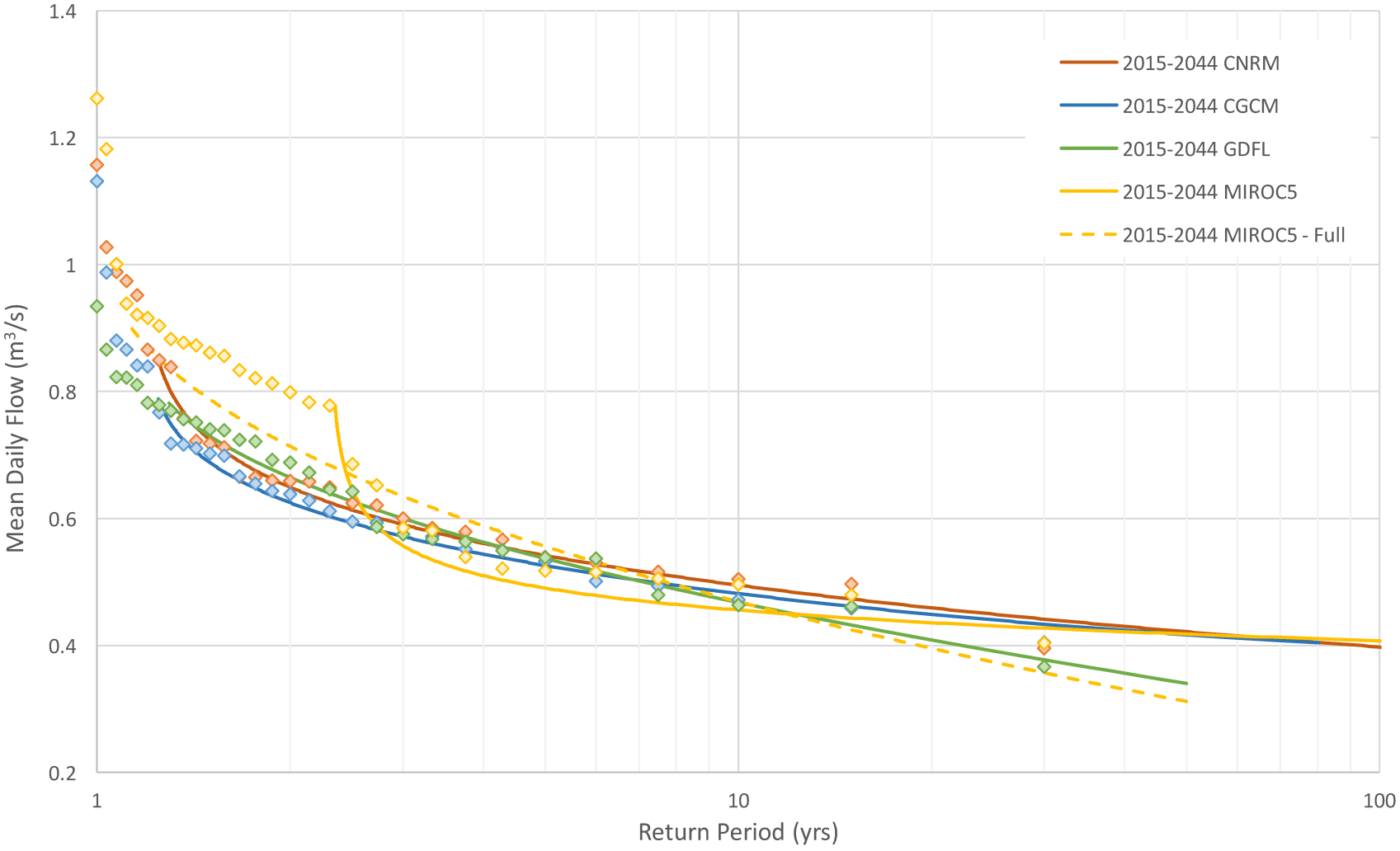

Figure 4.24 - Severity-duration-frequency curves for the annual 60-day summer/fall drought using four GCMs.

Chapter 5 Conclusion

This study successfully achieved its two objectives: to build a hydrological model for five watersheds in PEI, and use the model to assess the potential impact of climate change on the hydrological system. The hydrological model was built using a modified version of the HBV hydrological model running within the Envision alternative futures modeling framework. The hydrological model was calibrated by running a Monte Carlo simulation with 2000 runs and each run selecting a unique value for eleven model parameters from specified ranges using uniform distributions. The fit of the simulations was assessed using an objective function which incorporated the NSE and NSE_{ln} of streamflow and a weighted PBIAS term.

One parameter set was found to produce best-fit simulations for three of the six catchments, and ranked in the top ten in two other catchments, suggesting that the physical characteristics of all the watersheds are similar and one set of model parameters can be used to reasonably simulate all catchments in the study area. Four of the modeled catchments were satisfactorily calibrated, with monthly NSE values ranging from 0.61 to 0.76 and |PBIAS| values ranging from 0.01 to 0.21. A fifth catchment failed the monthly NSE test with a value of 0.43 and significantly lower OBJ scores, while the last was removed from the simulation due to consistently high volume errors which suggest that the model was unable to properly simulate the hydrological processes in this catchment, likely associated with municipal groundwater extraction for the City of Charlottetown. In general, the model was able to successfully simulate low-flow periods, while higher-flow periods in the fall and spring melt were timed appropriately but showed smoothed and elongated peaks with significantly reduced magnitudes compared to observed data.

Overall, the model shows that most aspects of the hydrology of PEI are not expected to change dramatically in the future. Mean annual drainage increases by 8% by 2035-44 over 1985-94, but up to 23% in the RCP2.6 scenario. However, the runoff coefficient is steady at 0.6 (±0.03 over time/scenario) and so the increased drainage is due to

increased precipitation. Evapotranspiration increases slowly but steadily in all scenarios, reaching 5% above baseline by 2035-44. The increased evapotranspiration comes at the expense of net recharge to deep groundwater, which decreases in all scenarios with a 60% (16mm) decrease for the baseline scenario but only a 15% decrease in wetter scenarios (MIROC5, RCP2.6). This may have significant consequences for groundwater levels in a region that is already facing significant challenges. Winter snowpack volumes also decrease drastically (-65%, -40% to -71%) in the last decade of simulation in all scenarios, likely associated with increases in winter temperature and shifting of winter precipitation to rain.

Seasonally, the increased flow is shown to occur in the winter (+38%, 28% to 50%), while spring melt flows drop by 12% (+4% to -22%) and summer flows show little change (+7%, -8% to +16%). Fall flows increase in wetter scenarios (RCP2.6 +23%, MIROC5 +33%) but drop in drier ones (RCP8.5 -12%). Annual flow indicators (Q10, Q50, Q90) remain stable in the base scenario (-2%, +1% to 0%), but show small but steady increases in all other scenarios (mean +6%, up to 13%, 12% and 11% respectively). Assessment of summer drought severity shows that there is little change to both the 7Q10 (-4%, -4% to +6%) and 60Q50 (-4%, -19% to +11%) droughts.

While climate change is often considered to be prone to uncertainty, this study compared results from six scenarios (three emission scenarios with one GCM and three other GCMs with one emission scenario) with MRI-CGCM3 RCP8.5 being the base-case scenario. The RCP2.6 scenario was consistently wetter than the base-case, with higher precipitation and flows throughout the year, while two of the comparison GCMs generated very similar results and the MIROC5 GCM produced slightly wetter and higher flow simulations. Change values between historic and future periods from the six simulations agree in direction for nearly all results, and show only moderate variation (generally less than 30 percentage points) in magnitude. This indicates that the impact of climate change on the hydrological system in PEI is relatively well constrained.

Chapter 6 Recommendations for Future Research

From this study, two major changes were identified that should be further investigated – large reductions in winter maximum snowpack volumes and net recharge to deep groundwater. In particular, the reduction in net recharge is concerning as PEI is highly dependent on groundwater for drinking water, and the province recently resumed issuing permits for groundwater withdrawal for irrigation which may put additional pressure on aquifers. Current aquifer extraction rates may not be sustainable with reduced net recharge, and should be further investigated.

Overall, while the magnitude of potential change to the hydrological system on PEI is moderate for most indicators and variation between scenarios is not extensive, the limitations to this study/model could mask significant change. In particular, human actions can have major impacts on climate and ecosystem, which can compound each other. For this reason, further work should be conducted to extend the model to fully utilize the power of the Envision alternative futures framework to assess how human actions, landscape management practices and adaptations may impact the results.

References

Abebe, N. a., Ogden, F. L., & Pradhan, N. R. (2010). Sensitivity and uncertainty analysis of the conceptual HBV rainfall-runoff model: Implications for parameter estimation. *Journal of Hydrology*, *389*(3–4), 301–310. http://doi.org/10.1016/j.jhydrol.2010.06.007

Aghakouchak, A., & Habib, E. (2010). Application of a Conceptual Hydrologic Model in Teaching Hydrologic Processes. *International Journal of Engineering Education*, *26*(4), 1–11. http://doi.org/0949-149X/91

Almorox, J., Quej, V. H., & Martí, P. (2015). Global performance ranking of temperature-based approaches for evapotranspiration estimation considering Köppen climate classes. *Journal of Hydrology*, *528*, 514–522. doi:10.1016/j.jhydrol.2015.06.057

Ahmad, H. M. N., Sinclair, A., Jamieson, R., Madani, A., Hebb, D., Havard, P., & Yiridoe, E. K. (2011). Modeling sediment and nitrogen export from a rural watershed in eastern Canada using the soil and water assessment tool. *Journal of Environmental Quality*, *40*(4), 1182–1194. doi:10.2134/jeq2010.0530

Baier, W. & Robertson, G. W. (1965). *Estimation of latent evaporation from simple weather observations*. Canadian Journal of Plant Science, 45: 276-284.

Bergström, S. (1976). Development and application of a conceptual runoff model for Scandinavian catchments. SMHI, Report No. RHO 7, Norrköping, 134 pp.

Bergström, S., & Graham, L. P. (1998). On the scale problem in hydrological modelling. *Journal of Hydrology*, *211*(1–4), 253–265. http://doi.org/10.1016/S0022-1694(98)00248-0

Beven, K. (1985). Distributed models. In: Anderson, M.G., Burt, T.P. (Eds.), Hydrological Forecasting, Wiley, New York, pp. 405–435.

Beven, K. (2001b). *Rainfall-runoff modelling : The primer*. Chichester, U.K. ; New York: J. Wiley.

Beven, K. (2001a). How far can we go in distributed hydrological modelling? *Hydrology and Earth System Sciences*, *5*(1), 1–12. http://doi.org/10.5194/hess-5-1-2001

Blöschl, G., & Montanari, A. (2010). Climate change impacts—throwing the dice? *Hydrological Processes*, *24*(3), 374–381. http://doi.org/10.1002/hyp.7574

Bone, C., Johnson, B., Nielsen-Pincus, M., Sproles, E., & Bolte, J. (2014). A Temporal Variant-Invariant Validation Approach for Agent-based Models of Landscape Dynamics. *Transactions in GIS*, *18*(2), 161–182. doi:10.1111/tgis.12016

Bootsma, A. (1994). Long term (100 yr) climatic trends for agriculture at selected locations in Canada. *Climatic Change*, *26*(1), 65–88. doi:10.1007/BF01094009

Boyer, C., Chaumont, D., Chartier, I., & Roy, A. G. (2010). Impact of climate change on the hydrology of St. Lawrence tributaries. *Journal of Hydrology*, *384*(1-2), 65–83. doi:10.1016/j.jhydrol.2010.01.011

Boyle, D. P., Gupta, H. V., Sorooshian, S., Koren, V., Zhang, Z., & Smith, M. (2001). Toward improved streamflow forecasts: Value of semidistributed modeling. *Water Resources Research*, *37*(11), 2749–2759. http://doi.org/10.1029/2000WR000207

Carpenter, T. M., & Georgakakos, K. P. (2006). Intercomparison of lumped versus distributed hydrologic model ensemble simulations on operational forecast scales. *Journal of Hydrology*, *329*(1–2), 174–185. http://doi.org/10.1016/j.jhydrol.2006.02.013

Chen, J., Brissette, F. P., Poulin, A., & Leconte, R. (2011), Overall uncertainty study of the hydrological impacts of climate change for a Canadian watershed, Water Resour. Res., 47, W12509, doi:10.1029/2011WR010602.

Chow, V. T. (1959). *Open-Channel Hydraulics*. McGraw-Hill.

Chow, V., Maidment, David R., & Mays, Larry W. (1988). *Applied hydrology* (McGraw-Hill series in water resources and environmental engineering). New York, N.Y.: McGraw-Hill.

Crossman, J., Futter, M. N., Oni, S. K., Whitehead, P. G., Jin, L., Butterfield, D., … Dillon, P. J. (2013). Impacts of climate change on hydrology and water quality: Future proofing management strategies in the Lake Simcoe watershed, Canada. *Journal of Great Lakes Research*, *39*, 19–32. doi:10.1016/j.jglr.2012.11.003

Dakhlaoui, H., Bargaoui, Z., & Bárdossy, A. (2012). Toward a more efficient Calibration Schema for HBV rainfall-runoff model. *Journal of Hydrology*, *444–445*, 161–179. http://doi.org/10.1016/j.jhydrol.2012.04.015

Dibike, Y. B., & Coulibaly, P. (2005). Hydrologic impact of climate change in the Saguenay watershed: Comparison of downscaling methods and hydrologic models. *Journal of Hydrology*, *307*(1-4), 145–163. doi:10.1016/j.jhydrol.2004.10.012

Dibike, Y. B., & Coulibaly, P. (2007). Validation of hydrological models for climate scenario simulation: the case of Saguenay watershed in Quebec. *Hydrological Processes*, *21*, 3123–3135. doi:10.1002/hyp.6534

Donner, L. J., and Coauthors, (2011). The dynamical core, physical parameterizations, and basic simulation characteristics of the atmospheric component AM3 of the GFDL global coupled model CM3. *Journal of Climate*, 24, 3484–3519.

Envision (2015). About Envision. Retrieved from http://envision.bioe.orst.edu/about.aspx

Fecko, P. A., & Johnson, B. J. (2008). Regional Channel Geometry Equations: A Statistical Comparison for Physiographic Provinces in the Eastern US. *River Research and Applications*, *24*, 823–834. doi:10.1002/rra.1080

Francis, R.M., (1989). Hydrogeology of the Winter River Basin, Prince Edward Island. P.E.I. Department of the Environment, Water Resources Branch, 117 p.

Inouye, A. M. (2014). Development of a Hydrologic Model to Explore Impacts of Climate Change on Water Resources in the Big Wood Basin, Idaho. Oregon State University.

IPCC, 2014: Climate Change 2014: Synthesis Report. Contribution of Working Groups I, II and III to the Fifth Assessment Report of the Intergovernmental Panel on Climate Change [Core Writing Team, R.K. Pachauri and L.A. Meyer (eds.)]. IPCC, Geneva, Switzerland, 151 pp.

Khakbaz, B., Imam, B., Hsu, K., & Sorooshian, S. (2012). From lumped to distributed via semi-distributed: Calibration strategies for semi-distributed hydrologic models. *Journal of Hydrology*, *418–419*, 61–77. http://doi.org/10.1016/j.jhydrol.2009.02.021

Kebede, A., Diekkrüger, B., & Moges, S. a. (2014). Comparative study of a physically based distributed hydrological model versus a conceptual hydrological model for assessment of climate change response in the Upper Nile, Baro-Akobo basin: a case study of the Sore watershed, Ethiopia. *International Journal of River Basin Management*, (May), 1–20. doi:10.1080/15715124.2014.917315

Kersebaum, K. C., Wurbs, A., de Jong, R., Campbell, C. A., Yang, J., & Zentner, R. P. (2008). Long-term simulation of soil-crop interactions in semiarid southwestern Saskatchewan, Canada. *European Journal of Agronomy*, *29*(1), 1–12. doi:10.1016/j.eja.2008.01.011

Kling, H., & Gupta, H. (2009). On the development of regionalization relationships for lumped watershed models: The impact of ignoring sub-basin scale variability. *Journal of Hydrology*, *373*(3–4), 337–351. http://doi.org/10.1016/j.jhydrol.2009.04.031

Krause, P., Boyle, D. P., & Bäse, F. (2005). Advances in Geosciences Comparison of different efficiency criteria for hydrological model assessment. *Advances in Geosciences*, *5*, 89–97.

Lindstrom, G., Johansson, B., Persson, M., Gardelin, M., & Bergström, S. (1997). Development and test of the distributed HBV-96 hydrological model. *Journal of Hydrology*, *201*(1-4), 272–288.

Ludwig, R., Chartier, I., Caya, D., Mauser, W., May, I., Turcotte, R., … Biner, S. (2009). The role of hydrological model complexity and uncertainty in climate change impact assessment. *Advances in Geosciences*, *21*(Journal Article), 63–71. http://doi.org/10.5194/adgeo-21-63-2009

Maloney, E. D., Camargo, S. J., Chang, E., Colle, B., Fu, R., Geil, K. L., … Zhao, M. (2014). North American climate in CMIP5 experiments: Part III: Assessment of twenty-first-century projections. *Journal of Climate*, *27*(6), 2230–2270. doi:10.1175/JCLI-D-13-00273.1

Martina, M. L. V, Todini, E., & Liu, Z. (2011). Preserving the dominant physical processes in a lumped hydrological model. *Journal of Hydrology*, *399*(1–2), 121–131. http://doi.org/10.1016/j.jhydrol.2010.12.039

Maurer, E. P., Hidalgo, H. G., Das, T., Dettinger, M. D., & Cayan, D. R. (2010). The utility of daily large-scale climate data in the assessment of climate change impacts on daily streamflow in California. *Hydrology and Earth System Sciences*, *14*(6), 1125–1138. http://doi.org/10.5194/hess-14-1125-2010

Mauser, W., & Bach, H. (2009). PROMET - Large scale distributed hydrological modelling to study the impact of climate change on the water flows of mountain watersheds. *Journal of Hydrology*, *376*(3–4), 362–377. http://doi.org/10.1016/j.jhydrol.2009.07.046

Moriasi, D. N., Arnold, J. G., Van Liew, M. W., Bingner, R. L., Harmel, R. D., & Veith, T. L. (2007). Model evaluation guidelines for systematic quantification of accuracy in watershed simulations. *Transactions of the ASABE*, *50*(3), 885–900. http://doi.org/10.13031/2013.23153

Nathan, R. J., & McMahon, T. A. (1990). Practical aspects of low flow frequency analysis. *Water Resources Research*, *26*(9), 2135–2141. http://doi.org/10.1029/90WR00534

Oni, S. K., Futter, M. N., Molot, L. a., Dillon, P. J., & Crossman, J. (2014). Uncertainty assessments and hydrological implications of climate change in two adjacent agricultural catchments of a rapidly urbanizing watershed. *Science of the Total Environment*, *473–474*, 326–337. http://doi.org/10.1016/j.scitotenv.2013.12.032

Pacific Climate Impacts Consortium, University of Victoria, (2014). Statistically Downscaled Climate Scenarios. Downloaded from https://www.pacificclimate.org/data/statistically-downscaled-climate-scenarios on 28 May 2016.

PEI Agriculture (2014). Report highlight agriculture's contribution to the Canadian economy. Retrieved from http://www.gov.pe.ca/agriculture/index.php3?number=1051387&lang=E

Quilbé, R., Rousseau, A. N., Moquet, J. S., Trinh, N. B., Dibike, Y., Gachon, P., & Chaumont, D. (2008). Assessing the effect of climate change on river flow using general circulation models and hydrological Modelling - Application to the Chaudière River, Québec, Canada. *Canadian Water Resources Journal*, *33*(1), 73–94. Retrieved from http://www.scopus.com/inward/record.url?eid=2-s2.0-38849150190&partnerID=40&md5=560bb818b5ff87a555a67a49b237d902

Reed, S., Koren, V., Smith, M., Zhang, Z., Moreda, F., & Seo, D. J. (2004). Overall distributed model intercomparison project results. *Journal of Hydrology*, *298*(1–4), 27–60. http://doi.org/10.1016/j.jhydrol.2004.03.031

Rivard, C., Paniconi, C., Vigneault, H., & Chaumont, D. (2014). A watershed scale study of climate change impacts on groundwater recharge (Annapolis Valley, Nova Scotia,

Canada). *Hydrological Sciences Journal*, *59*(8), 1437–1456. http://doi.org/10.1080/02626667.2014.887203

Roberts, J., Pryse-Phillips, A., & Snelgrove, K. (2012). Modeling the Potential Impacts of Climate Change on a Small Watershed in Labrador, Canada. *Canadian Water Resources Journal*, *37*(3), 231–251. doi:10.4296/cwrj2011-923

Salathé, E. P. (2005). Downscaling simulations of future global climate with application to hydrologic modelling. *International Journal of Climatology*, *25*(4), 419–436. http://doi.org/10.1002/joc.1125

Samuel, J., Coulibaly, P., & Metcalfe, R. a. (2012). Identification of rainfall-runoff model for improved baseflow estimation in ungauged basins. *Hydrological Processes*, *26*(May 2011), 356–366. doi:10.1002/hyp.8133

Santelmann, M., McDonnell, J., Bolte, J., & Chan, S. (2012). Willamette water 2100 : river basins as complex social-ecological systems. *WIT Transactions on Ecology and The Environment*, *155*, 575–586. doi:10.2495/SC120481

Seibert, J. (1999). Regionalisation of parameters for a conceptual rainfall-runoff model. *Agricultural and Forest Meteorology*, *98–99*, 279–293. http://doi.org/10.1016/S0168-1923(99)00105-7

Seibert, J., & McDonnell, J. J. (2010). Land-cover impacts on streamflow: a change-detection modelling approach that incorporates parameter uncertainty. *Hydrological Sciences Journal*, *55*(3), 316–332. doi:10.1080/02626661003683264

Seibert, J., & Vis, M. J. P. (2012). Teaching hydrological modeling with a user-friendly catchment-runoff-model software package. *Hydrology and Earth System Sciences*, *16*, 3315–3325. doi:10.5194/hess-16-3315-2012

Sheffield, J., Barrett, A. P., Colle, B., Fernando, D. N., Fu, R., Geil, K. L., … Yin, L. (2013). North American Climate in CMIP5 experiments. Part I: Evaluation of historical simulations of continental and regional climatology. *Journal of Climate*, *26*(23), 9209–9245. doi:10.1175/JCLI-D-12-00592.1

Statistics Canada, (2011). 2011 Census of Agriculture. Retrieved from http://www.statcan.gc.ca/eng/ca2011/index

Steele-Dunne, S., Lynch, P., McGrath, R., Semmler, T., Wang, S., Hanafin, J., & Nolan, P. (2008). The impacts of climate change on hydrology in Ireland. *Journal of Hydrology*, *356*(1–2), 28–45. http://doi.org/10.1016/j.jhydrol.2008.03.025

Taylor, K. E., R. J. Stouffer, and G. A. Meehl, 2012 : An overview of CMIP5 and the experiment design. Bull. Amer. Meteor. Soc., 93, 485–498.

Tu, J. (2009). Combined impact of climate and land use changes on streamflow and water quality in eastern Massachusetts, USA. *Journal of Hydrology*, *379*(3-4), 268–283. doi:10.1016/j.jhydrol.2009.10.009

Waldick, R. (2011). Integrated Landscape Assessment and Decision-Support Process and Tool Kit for Mainstreaming Climate Change - Application in Southeastern Ontario. Briefing Document.

Watanabe, M., and Coauthors, (2010) Improved climate simulation by MIROC5: Mean states, variability, and climate sensitivity. *Journal of Climate*, 23, 6312–6335.

Werner, A. T., & Cannon, A. J. (2015). Hydrologic extremes – an intercomparison of multiple gridded statistical downscaling methods. *Hydrology and Earth System Sciences Discussions*, *12*(6), 6179–6239. http://doi.org/10.5194/hessd-12-6179-2015

Vache, K. (2015). Flow Documentation. Retrieved from http://envision.bioe.orst.edu/Documents/

Velázquez, J. A., Schmid, J., Ricard, S., Muerth, M. J., Gauvin St-Denis, B., Minville, M., … Turcotte, R. (2013). An ensemble approach to assess hydrological models' contribution to uncertainties in the analysis of climate change impact on water resources. *Hydrology and Earth System Sciences*, *17*(2), 565–578. http://doi.org/10.5194/hess-17-565-2013

Voldoire, A., and Coauthors, (2013) The CNRM-CM5.1 global climate model: Description and basic evaluation. *Climate Dynamics*, 40, 2091–2121, doi:10.1007/s00382-011-1259-y

Yapo, P. O., Gupta, H. V., & Sorooshian, S. (1996). Automatic calibration of conceptual rainfall-runoff models: sensitivity to calibration data. *Journal of Hydrology*, *181*(1–4), 23–48. http://doi.org/10.1016/0022-1694(95)02918-4

Yukimoto, S., and Coauthors, (2012). A new global climate model of the Meteorological Research Institute: MRI-CGCM3— Model description and basic performance. *Journal of the Meteorological Society of Japan*, 90A, 23–64.

Zégre, N., Skaugset, A. E., Som, N. A., McDonnell, J. J., & Ganio, L. M. (2010). In lieu of the paired catchment approach: Hydrologic model change detection at the catchment scale. *Water Resources Research*, *46*(11), 1–20. http://doi.org/10.1029/2009WR008601

Zhang, X., & Lindström, G. (1997). Development of an Automatic Calibration Scheme for the HBV Hydrological Model. *Hydrological Processes*, *11*, 1671–1682.